RESEARCH and TECHNOLOGY

Annual Report 1984

LEWIS RESEARCH CENTER

(NASA-TM-86899) [RESEARCH AND TECHNOLOGY HIGHLIGHTS OF THE LEWIS RESEARCH CENTER] Annual Report, 1984 (NASA) 52 p
HC A04/MF A01 CSCL 05A

N85-17928

Unclas
G3/99 01401

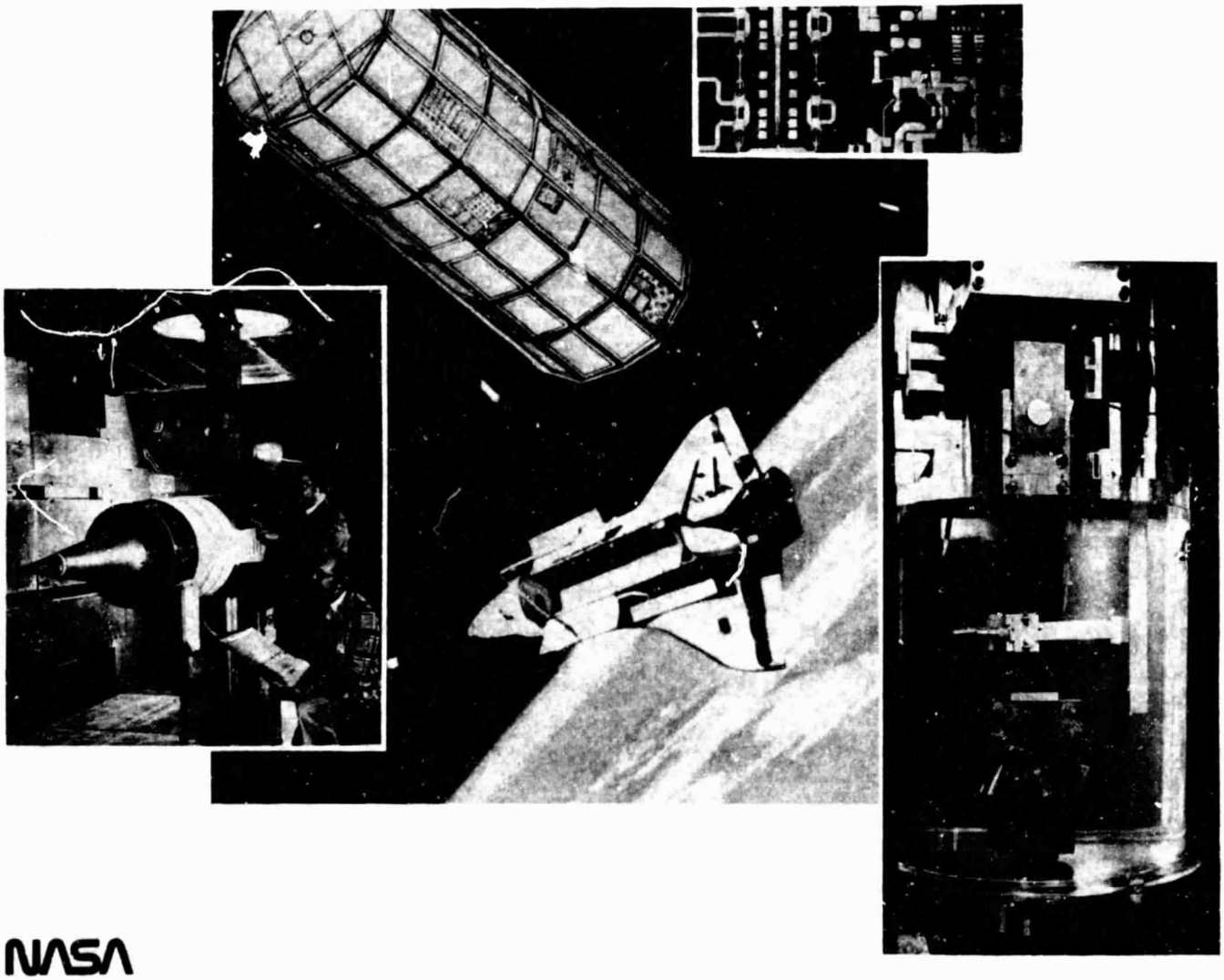

NASA
National Aeronautics and Space Administration

NASA Technical Memorandum 86899

Contents

Introduction

This report presents highlights of research accomplishments of the Lewis Research Center for fiscal year 1984. The report is divided into four major sections covering aeronautics, space communications, space technology, and materials and structures. Six articles on energy are included in the space technology section.

The results of all research and technology work performed during the fiscal year are contained in Lewis-published technical reports and presentations prepared either by Lewis scientists and engineers or by contractor personnel. In addition, significant results are presented by university faculty or graduate students in technical sessions and in journals of the technical societies.

In 1984, four Lewis products were selected for the Research & Development Magazine IR-100 awards. All four are described and identified in this report. In addition, the Lewis Distinguished Paper for 1983-84, which was selected by the Chief Scientist and a Research Advisory Board, is included and so identified.

For general information about this report, contact Robert W. Graham at (216) 433-4000, Ext. 6146, or FTS 294-6146.

Aeronautics

Three-Component Velocity Measurements Using Fabry-Perot Interferometer

The measurement of the three-dimensional gas velocity vector is needed in many fluid mechanics experiments. Because of its nonintrusive nature laser anemometry is frequently used for these measurements. However, the velocity vector is difficult to measure in high-speed flows with a conventional fringe type of laser anemometer if only a single viewing port is available.

A new method of measuring the mean velocity vector was developed that uses a backscatter optical system and a single laser beam. The Doppler-shifted frequency of laser light scattered from small particles in the flow is measured with a scanning, confocal Fabry-Perot interferometer interfaced to a small computer. The mean velocity magnitude and flow direction are determined by using a parameter estimation procedure. Analysis of the technique, confirmed by measurements made in a 320-m/s air jet, showed an uncertainty in the measured velocity magnitude of about 1 percent and in the flow direction of about 1°.

Formulation of Blade-Flutter Spectral Analyses in Stationary Reference Frame

It was shown recently that blade-flutter vibratory characteristics can be obtained from casing-mounted sensor measurements. Two types of sensors were employed: an optical blade-tip displacement sensor and a high-response static-pressure transducer. The main advantage of these transducers over rotor-mounted gauges is that all of the blades can be surveyed with a single transducer. However, the analysis of signals from these transducers is more complicated.

All aspects of spectral analysis of signals from stationary sensors have been mathematically documented in a unified way. The derivations were carried out in the discrete domain and the only restriction imposed on flutter frequency was that it be less than the blade passing frequency.

The complete unsteady pressure field in a fixed frame of reference was analytically represented by sampling at a rate that is a multiple of the blade passing frequency. This allowed the pressure spectrum to be interpreted and transformed into the rotating frame of reference.

To determine the true flutter frequency with casing-mounted sensors requires that two sensors be placed at different circumferential locations. However, this angular separation is not arbitrary. It must satisfy certain conditions that depend on the sampling rate. These conditions were derived for the representative sampling rates for each type of sensor. Mathematical representation was also obtained for a contribution to the total unsteady pressure signal that arises because of the interaction of the steady-state pressure field and the unsteady blade-displacement field. This interaction must be taken into account when interpreting the unsteady pressure spectra.

The report describing this research was selected as the Lewis Distinguished Paper for 1984.

Laser Speckle Photography for High-Temperature Strain Measurements

To make more durable components for the hot sections of turbine engines, a method for measuring strain in metal structures at temperatures of 1600 to 1800 °F is needed. The conventional sensor for measuring strain in metal structures is the electrical resistance strain gauge. Currently available strain gauges can measure fluctuating strain to 1800 °F, but for measurements of steady strain where a repeatable zero-strain reference must be maintained, such strain gauges are limited to temperatures below 700 °F.

An alternative approach to strain measurements is an optical technique in which dimensional changes in a structure are determined from photographs of the surface of the structure. The technique, which is being investigated at United Technologies Research Center under a Lewis

contract, is based on the speckle pattern that is formed when a surface is illuminated with laser light. Comparing photographs of the speckle patterns taken before and after dimensional changes can reveal changes as small as a few parts per million (called microstrain). The comparison is made with laser light in such a way that the slightly displaced speckle patterns form interference fringes.

Thermal and mechanical strains have been measured on samples of a common material used in jet engine combustor liners that were heated from room temperature to 870 °C and then cooled to 220 °C in a laboratory furnace. The physical geometry of the sample surface was recorded at selected temperatures by means of a set of 12 single-exposure specklegrams. Sequential pairs of specklegrams were compared in a heterodyne interferometer, which allowed high-precision measurement of differential displacements. Good speckle correlation was also observed between the first and last specklegrams. This showed the durability of the surface microstructure and permitted a check on accumulated errors. Agreement with calculated thermal expansion was to within a few hundred microstrain over a range of 14 000.

Fiber Optic Combustor Viewing System

Considerable emphasis is being placed on improving the durability of hot-section components of aircraft turbine engines in order to reduce maintenance costs. One of the critical components is the combustor liner. The fiber optic viewing system provides views of the interior of combustors during testing so that anomalous operation and incipient failures can be identified. Such a system will enhance the capability for correlating cause-and-effect relationships for combustor liner failure and will thus lead to more durable combustors.

This system was developed by United Technologies Research Center under contract to Lewis. The system consists of a water-cooled optical probe, an actuator to position the probe within the combustor, fiber optic cables to transfer images out of the probe and to illuminate the probe, an optical interface unit containing cameras and light sources, and a remote control panel. Images can be obtained either with illumination from the burner flame or with external illumination. Pulsed laser light coupled with narrow-band filters and a suitable short-exposure shutter permits images normally obscured by the luminous flame. This capability was demonstrated in preliminary tests; it is not yet incorporated in prototype systems. Probes with different viewing angles and a variety of viewing lenses provide for different fields of view and image resolution.

Application of Infrared Photography to Turbine Vane Temperature Mapping

An infrared photography technique has been used to measure the surface temperature distribution on turbine vanes operated in a high-pressure turbine test facility. A specially designed fiber optic probe with water cooling for protection (from the severe environment) was developed to transfer images of the vanes from inside the test rig to an external infrared camera. The recorded images are analyzed with a digital image processor to map contours of constant film density. The film density is proportional to vane surface temperature. By including one surface temperature measurement within the field of view, actual temperatures can be assigned to each level of film density.

Air-cooled vanes have been tested at gas temperatures to 2300 °F and pressures to 300 psi. Vane surface temperatures ranged from 1200 to 1600 °F. The water-cooled fiber optic probe can be traversed into the gas stream and rotated over ±45° so as to obtain images from seven vanes. Test facilities such as this enable the measurement of the cooling effectiveness of different vane-cooling designs and lead to optimum cooling of vanes with a minimum amount of cooling air. Minimizing cooling air requirements leads to improved fuel economy.

Flow Measurements in Internal Combustion Engines

Because of its nonintrusive nature, laser Doppler velocimetry (LDV) has become a valuable tool for air velocity measurements in an internal combustion engine. Using the system now operational at Lewis, researchers have made simultaneous multicomponent measurements of the airflow within a piston-cylinder assembly. The unique feature of this five-beam LDV system is the ability to simultaneously measure three components of velocity by using a single optical access port and one focusing lens. The technique for measuring the on-axis component of velocity was developed by TSI, Inc.

The results of this experimental work are being used to validate and refine a multidimensional numerical simulation of the airflow within the piston-cylinder assembly of interest. The ultimate goal of this work is to improve the efficiency of a two-stroke diesel aircraft engine.

IR-100 Computer Program for Rotordynamic Analysis

ARDS (analysis of rotordynamic systems) is a finite-element-based computer program that analyzes the free and forced response of multishaft rotor-bearing systems. It was selected by Research & Development Magazine as one of the best new products of 1984. Among the analyses that ARDS can perform are stability of system whirl modes; transient response to sudden unbalance, turns, and lateral acceleration; peak response due to suddenly applied unbalance; and sensitivity of response to changes in rotor parameters. Results are automatically plotted and printed.

The analysis is based on the concept of component mode synthesis, or substructuring, to obtain a reduced set of coupled system equations. These equations may be either solved

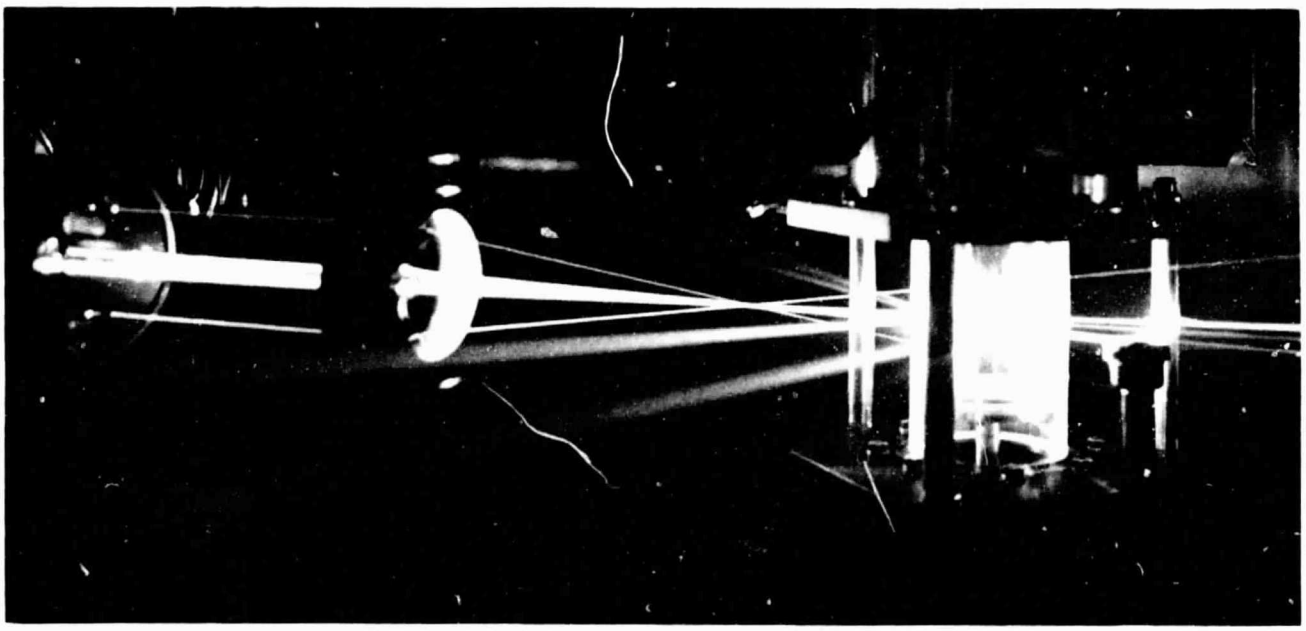

LDV flow measurements

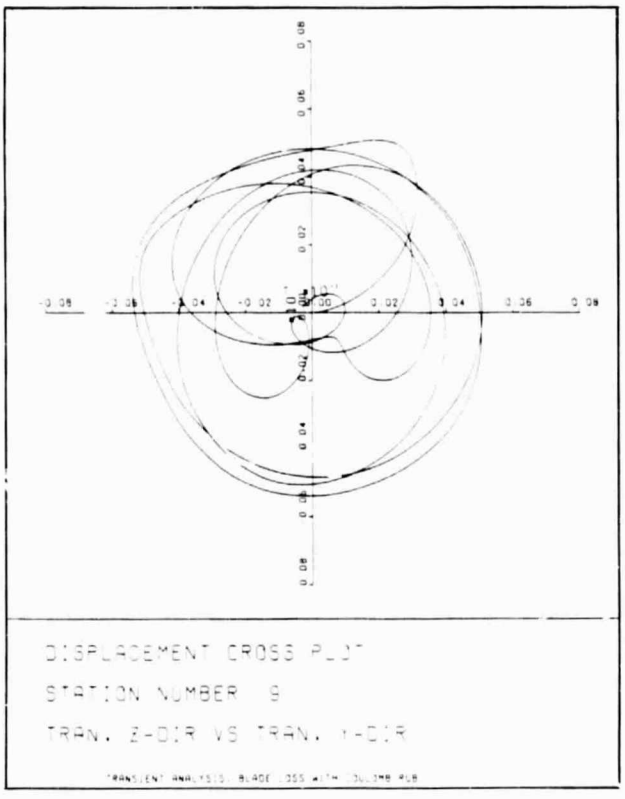

Example of ARDS output

for steady-state system response or integrated forward in time to obtain transient response. Nonlinear shaft interconnections and support bearings can be accurately modeled. ARDS is a Fortran program that will run on most mainframe computers. Input follows the usual form for rotordynamic codes with only shaft and bearing properties required. No auxiliary program (such as NASTRAN) is required.

AESOP—A Program for Computer-Aided Design of Linear Multivariable Control Systems

AESOP is an interactive computer program that solves linear quadratic regulator (LQR) and Kalman filter problems for linear, time-invariant systems described in state-space form. In addition to LQR and filter design, AESOP performs open-loop system analyses (eigenvalues, eigenvectors, residues, and controllability and observability checks), determines system response to noise inputs (covariance matrices), computes system transient responses (open and closed loop), and finds transfer functions and frequency responses (poles, zeroes, and Bode plots). Calculations done by AESOP are defined in terms of numbered functions. The user requests a function by entering its assigned function number. The numbers can be entered singly (in an interactive mode) or as a string (in a batch mode) as desired. To aid the user, AESOP checks the validity of all requested function number sequences. Graphics output is provided for displaying transient and frequency responses.

AESOP is written in ANSI-66 Fortran for running on an IBM 370/3033 with a TSS/370 operating system. The main program is dimensioned to handle 50th-order systems, with the largest problem run being 41st order. Object code requires about 200K bytes, with an additional 1.7M bytes required for matrix storage. All Fortran source code is provided with the exception of basic graphics package subroutines.

Real-Time Multiprocessor Simulator

RTMPS is a parallel-processor system developed to provide real-time nonlinear simulations for control system studies. It consists of a number of commercially available microcomputers. Each microcomputer is assigned a portion of the simulation equations to solve. By using parallel processing and specially designed software, the simulation equations can be solved in less time than it would take if a single microcomputer were used. It is therefore possible to configure a low-cost simulator that can provide the real-time solutions required when a simulator is to be interfaced with actual control system hardware.

Software tools have been developed for the RTMPS that automate the process of dividing up the equations for parallel processing, allow the RTMPS to be programmed in a high-level

language, and provide for convenient, interactive operation. This software represents a unique, user-friendly environment for real-time simulation. The RTMPS concept and associated software tools can be applied to a variety of simulator configurations and microcomputer types. All software has been developed by Lewis personnel and will be available with documentation after system testing.

Influence of Stator Endwall Contouring on Performance of Small Turbines

Small axial turbines are less efficient than large turbines, largely because of Reynolds number and size effects. One concept that has the potential for increasing small turbine efficiency is stator endwall contouring. An experimental and analytical stage evaluation of stator endwall contouring was conducted in which two differently contoured stator configurations were investigated and their performance compared with that of a reference cylindrical-endwall stator. A common rotor was used with all three stator configurations. The first contoured stator configuration had an S-shaped tip endwall profile and the second configuration had a conical-convergent tip endwall profile. The two contoured stator configurations improved stage efficiency by about 0.7 point. Subsequent loss analysis indicated that this improvement was due primarily to reduced stator loss, particularly lower stator blade and endwall friction losses.

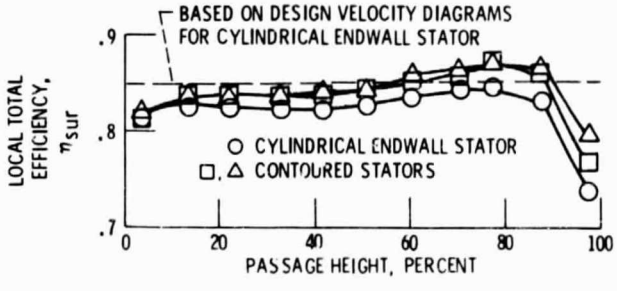

Effect of stator endwall contouring on turbine performance

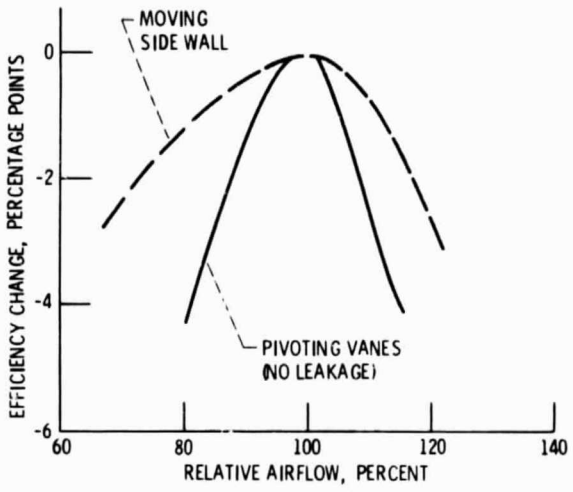

Effect of variable-area radial turbine on efficiency

Variable-Area Radial Turbine

Part-power fuel consumption of rotorcraft engines can be reduced by operating the engine components at or near their peak efficiency while the engine power is modulated by changing the airflow. A key component to the success of this engine is a viable high-temperature, variable-geometry turbine. A radial turbine with a translating stator side wall is one of the concepts being studied. Tests of this concept showed that moving the stator side wall is a viable method to efficiently vary the flow capacity of a radial turbine. Comparing the performance of this turbine with that of a pivoting-vane radial turbine showed that the peak efficiencies of both turbines were equal but that the loss in efficiency of the moving-side-wall turbine was less as the stator area was changed.

Turbine Bypass Engine

Many aircraft that require wide variations in power have difficulty in maintaining efficient engine operation at extreme power settings. A fighter aircraft may require large engines and high power for supersonic climb or combat but spends most of its mission at subsonic cruise or loiter, where the engine power requirement is much lower. At these low power settings the engine airflow and

rotational speed must be reduced. This lowers engine efficiency and causes large penalties in fuel consumption. One means of alleviating this problem is with a variable-area turbine, which provides a variable turbine airflow capability. But this adds complexity, cost, maintenance, and reliability problems in the engine hot section.

A simpler scheme is the turbine bypass system. In this concept the turbine area is fixed and designed for part power and maximum airflow. At high power, some of the airflow is bypassed around the turbine so as to maintain the required turbine airflow. With this system, maximum engine airflow and rotational speed can be maintained over a wide range of throttle settings. In-house and contracted studies have shown that a future supersonic transport engine could use 10 percent less fuel than a more conventional engine. Related studies for fighter aircraft have shown that a single-spool turbojet with a turbine bypass system would have a 30 percent lower production cost than mixed-flow afterburning turbofans. Additional studies are planned to evaluate the turbine bypass concept over a wider range of applications.

Topping-Cycle Engine

A novel aircraft gas turbine engine system that uses hydrogen fuel was analytically investigated and compared with a conventional (baseline) turboshaft engine. This novel aircraft engine, called the topping-cycle engine, could be considered for future transport aircraft systems that use hydrogen (or methane) as a fuel. The topping-cycle engine consists of a main turboshaft engine mechanically coupled to an auxiliary power generation loop that augments the power output of the main engine. A fraction of the compressor airflow in the main engine (about 20 percent) is bled off and fed into the auxiliary power generation loop. The total engine fuel flow is fed directly into the auxiliary loop combustor. Thus the auxiliary loop combustor operates in a highly fuel-rich state, with an equivalence ratio between 2.5 and 4.5. Since only a fraction of the total fuel flow is burned in the auxiliary loop, the combustion products from this

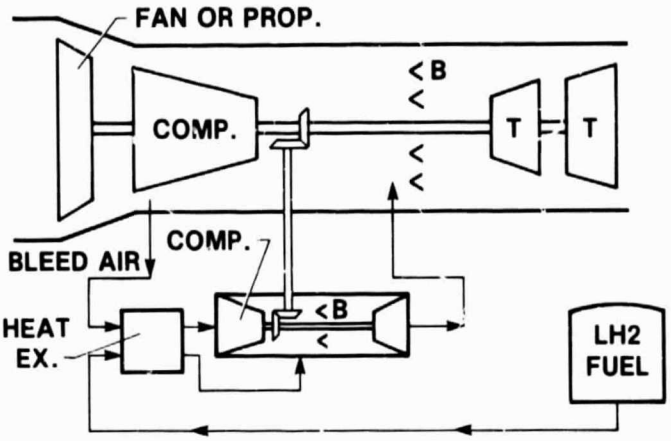

Topping-cycle engine

loop include unburned hydrogen fuel, nitrogen, and water vapor. These fuel-rich products are expanded through the auxiliary loop turbine and ducted directly into the main engine combustor. There the fuel mixture is combined with excess air, burned completely, and expanded through the main engine turbine.

Analyses indicated that the performance of a topping-cycle engine would be 12 to 20 percent better than that of the baseline turboshaft engine—depending on design cycle pressure ratio. Calculations also indicate that a topping-cycle engine would weigh about the same as a conventional engine. The comparison was made for a 10 000-hp turboshaft engine.

Low-Speed Aeroacoustic Performance of a Supersonic Axisymmetric Mixed-Compression Inlet

Supersonic cruise inlets are designed to provide optimum performance at cruise conditions. As a result, the inlet cowl lip is sharp, bleed systems are incorporated in the design, and the inlet capture area is smaller than that required at takeoff conditions. Therefore auxiliary inlet systems are needed to provide the additional

engine airflow required at takeoff and approach, where acoustic analysis shows forward-propagated fan noise to be prominent. These additional openings in the inlet nacelle could provide paths for the propagation of fan-generated noise; inflow bleed could also affect noise generation and propagation. Aerodynamically, because of the internal flow characteristics of supersonic inlets at low speed, large performance penalties could result from lip flow separation and from inflow bleed.

Reductions in propagated fan noise levels are highly desirable and can be accomplished through inlet choking techniques and careful design of auxiliary inlet systems. Use of variable-geometry techniques could reduce lip flow separation and improve inlet performance. An experimental program was established to verify these techniques and design concepts at ground static and low-speed conditions. Participants in this program were NASA Lewis and NASA Langley and three contractors: Boeing, Lockheed, and Douglas. Each participant (except Langley) was to design, fabricate, and test auxiliary inlet systems that would be representative of their auxiliary inlet concepts and be adapted to the existing inlet model system. The NASA Ames P-inlet model was selected for this investigation. Its design is representative of proposed supersonic cruise inlet designs, and auxiliary inlet systems could be easily accommodated. The inlet system was coupled to a JT8D refan simulator powered by an air turbine. The fan simulator provided characteristic fan noise signatures and pumped the airflow through the inlet. The P-inlet model with the NASA Lewis auxiliary doors was tested in the Lewis 9- by 15-Foot Anechoic Wind Tunnel at Mach 0, 0.1, and 0.2.

The testing was completed at Lewis in September 1984. Preliminary performance results indicate that both centerbody and cowl bleed systems should be sealed to prevent bleed system backflow for all low-speed operations as bleed system backflow was found to be severely detrimental to inlet performance. Performance was significantly degraded by high cowl lip Mach numbers (due to sharp lip flow separations) and

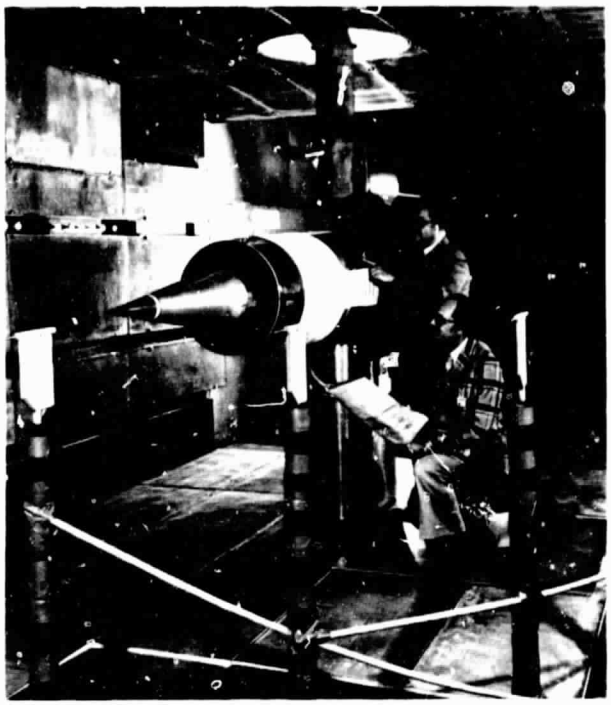

P-inlet model in tunnel

by high throat or auxiliary door Mach numbers. Therefore a centerbody position that tends to equalize the cowl lip and throat flow areas seems to be optimum.

Preliminary acoustic results at Mach 0.2 indicate that the open auxiliary doors increased the tonal content at the fan source, probably because of flow distortions. However, the open doors did not provide a significant additional noise path. The supersonic inlet greatly suppressed fan multiple-pure-tone generation at the fan source. In addition, numerous strong tones in the spectra were associated with the bleed system. These tones were not fan related but did change with centerbody position and bleed configuration.

Buoyancy Effect on Laminar Heat Transfer in a Rotating Tube

Laminar heat transfer was analyzed in a tube rotating about an axis perpendicular to the tube axis. The solution applies for flow in the tube that

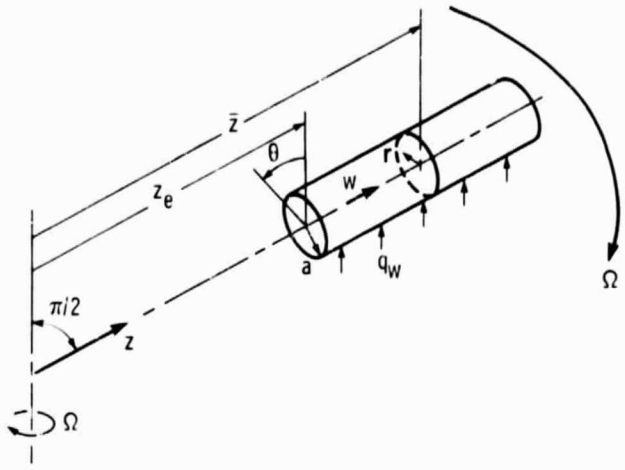

Heated tube rotating about a perpendicular axis

is either radially outward from, or radially inward toward, the axis of rotation. The conditions are fully developed and there is uniform heat addition at the tube wall. The analysis was performed by using the Taylor number as a perturbation parameter to expand velocities and temperature in power series. Coriolis and buoyancy forces caused by tube rotation were included, and the solution was calculated through second-order terms. The secondary flow induced by the Coriolis terms always tends to increase the heat-transfer coefficient; this effect can dominate when the heating at the wall is small. For radial inflow the buoyancy effects also tend to improve heat transfer since buoyancy is acting toward the axis of rotation. For radial outflow, however, bouyancy tends to reduce heat transfer; for large wall heating the buoyancy effect can dominate and there is a net reduction in heat transfer coefficient.

Experiments and Modeling of Dilution Jet Flow Fields

The proper thermal conditioning of the products of combustion in gas turbine engines is accomplished by dilution with air. This process influences the average temperature level and uniformity of the gases leaving the combustor. The costly and time-consuming task of controlling or tailoring the exit temperature profiles through cut-and-try testing can be reduced with the aid of computer models capable of characterizing the exit distribution in terms of the upstream flow and geometric variables.

In its simplest geometry the dilution process can be portrayed as a row of jets penetrating normally into a straight duct flow. In 1972-75, the Aerojet Liquid Rocket Company, under contract to Lewis, performed an extensive experimental study of this configuration and developed an empirical model for predicting the temperature distribution that was based on assumed vertical profile similarity. Beginning in 1979, the Garrett Turbine Engine Company, under contract to Lewis, obtained experimental data and extended the existing empirical model to include effects of several flow and geometric variations typical of most gas turbine combustors.

Temperature field measurements for selected experiments from the Garrett study have recently been compared with distributions calculated with the empirical model and with a three-dimensional elliptic code using a standard k-ϵ turbulence model. The empirical model provides very good quantitative predictions of the temperature field within the parameter range of the generating experiments whenever the primary assumptions in the model are supported by the experimental data. Although the numerical model calculations consistently exhibit too little mixing, the trends that result from varying the independent flow and geometric variables, as observed in the experimental data, are approximated correctly.

Three-dimensional codes with improved numerics, accuracy, and turbulence models should provide more quantitative predictions. It is significant that the three-dimensional codes can provide calculations for complex flows that are outside the range of available experiments or for which the assumptions in the empirical model are known *a priori* to be invalid. Also important is the fact that the three-dimensional codes predict all flow-field quantities (i.e., velocity, turbulence, etc.) and not just those that have been empirically modeled.

Compressor Blade Row Interactions

Computer codes that are currently used to design compressor and turbine blade rows and to predict flow fields through these blade rows assume that the flow is steady in time. However, it is well known that the flow around turbomachinery blades is highly unsteady because of interactions between moving rotor blade rows and stationary stator blade rows. Improvements in current design and analysis capabilities will therefore require a better understanding of the unsteady flow phenomena generated by blade row interactions. Initial measurements in the unsteady flow field within a compressor stator operating downstream of a transonic fan rotor have recently been obtained by laser anemometry.

Contour plots have been made of the turbulent energy distribution in the stator at one instant in time. The results show that rotor blade wakes are chopped by the stator blades and indicate that current wake transport models, which assume that the rotor wakes pass through the stator with relatively little distortion of the wake shape, are not adequate to describe the dynamics of the blade row interaction process. Data obtained at additional times during the blade passing cycle are being analyzed in order to develop a complete picture of the wake dynamics and its effect on the stator flow field. Future measurements will attempt to determine the coupling between the flow field dynamics and the unsteady stator surface pressure conditions.

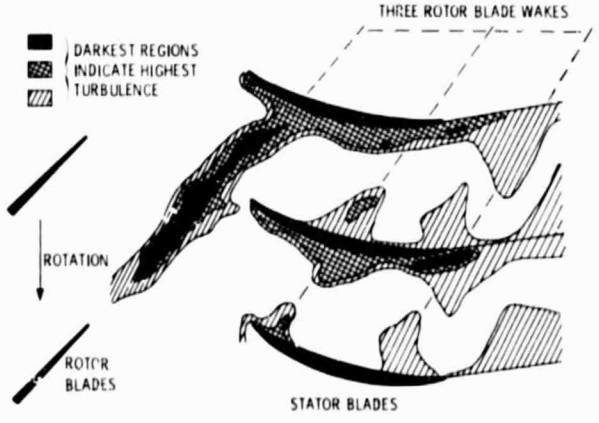

Compressor blade row interactions

Model Equation for Simulating Flows in Multistage Turbomachinery

The flow field in multistage compressors and turbines is extremely complex. This flow field is highly unsteady, with time scales ranging from a fraction of shaft speed to several times that of the highest blade passing frequency. The length scales of the flow are also diverse. They range from the circumference of the machine to a fraction of a blade chord. The vast range of time and length scales makes the problem of direct numerical simulation practically impossible. Confronted with analyzing complex, multiple-scale problems, aerodynamicists have traditionally described their physics in terms of an appropriately averaged set of equations. A prime example of this methodology is the Reynolds-averaged modeling of turbulent flows. For turbomachinery the literature seems to support a description based on an average blade passage. With respect to a given blade row, the flow within the average passage is steady and spatially periodic from blade passage to blade passage.

A rigorous attempt has been made to derive the equations governing this flow field. The derived equation set provides a reference against which multistage analyses can be judged for their completeness. In particular, given the advances made in the field of computational fluid dynamics to solve a similar set of equations, a numerical simulation based on a properly scaled version of these equations should provide a more fundamental base for the analysis of turbomachinery flow than currently exists.

Turbulent Solutions of the Equations of Fluid Motion

Most fluid flows, including those occurring in nature and those that are manmade, are turbulent. Several turbulent solutions of the unaveraged Navier-Stokes equations (equations of fluid

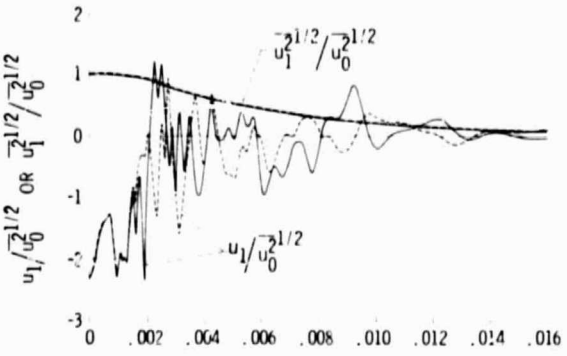

Calculated evolution of turbulent velocity fluctuations

motion) have been obtained. Those equations were solved numerically in order to study the nonlinear physics of incompressible turbulent flow. Three-dimensional cosine velocity fluctuations were used for the initial conditions; the boundary conditions were assumed to be periodic. The three components of the mean-square velocity fluctuations were initially equal. The solutions show characteristics of turbulence, including the linear and nonlinear excitation of small-scale fluctuations. For the stronger fluctuations the initially regular flow developed into an apparently random turbulence; this suggests that randomness can arise as a consequence of the structure of the Navier-Stokes equations. The apparent randomness of the instantaneous fluctuations is shown by their sensitive dependence on initial conditions. The turbulence considered included isotropic, anisotropic, homogeneous, and inhomogeneous cases; a mean shear was sometimes present. Turbulence processes studied include the transfer of energy between eddy sizes and between directional components and the production, dissipation, and spatial diffusion of turbulence. It was concluded that numerical methods can be used to profitably study the physical processes in turbulence.

Analytical Modeling of Circuit Aerodynamics in New Altitude Wind Tunnel

Lewis is planning to modify and rehabilitate the Altitude Wind Tunnel (AWT) to provide a unique national subsonic (Mach 0.1 to 1.0) propulsion, icing, and aeroacoustic facility. To verify that such a tunnel is feasible, a preliminary design study has been started. As part of this study, intensive experimental and analytical modeling programs have begun. The modeling effort will assess the performance of the new AWT design, study the inevitable problems that will arise, and investigate proposed design changes. The experimental program primarily uses 1/10th-scale component and complete loop models that are faithful representations of the full-scale facility. Axisymmetric and three-dimensional viscous computer codes are being used to analyze the flow through the various AWT components. The development of these codes has allowed a more sophisticated analytical modeling program to be undertaken than had been possible.

An important consideration in the design of a new wind tunnel is the test-section flow quality. One measure of this is the distortion level, defined as the difference between the maximum and minimum velocity (outside the boundary layer) divided by the average velocity. In the new AWT a distortion level of 0.025 or lower was desired at the design test-section Mach number of 0.8. A computer code called VISTA, which solves an approximate form of the Navier-Stokes equations by forward marching in space, was

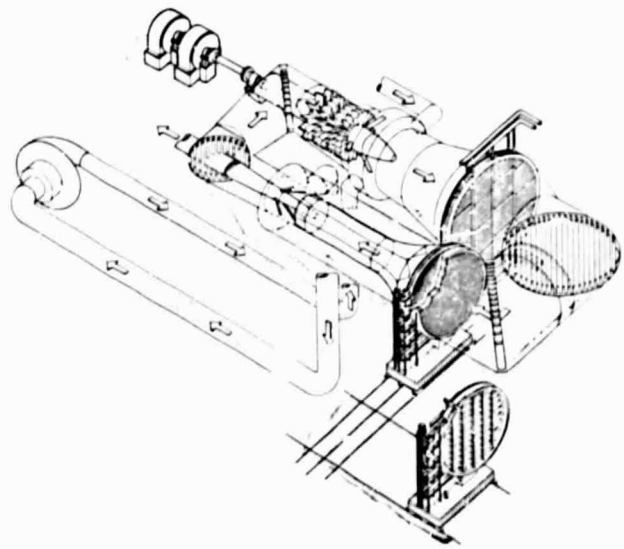

Schematic of AWT

used to compute the distortion over a range of test-section Mach numbers. For the Mach 0.8 condition, the predicted distortion level was 0.014 at the bellmouth exit, falling to less than 0.001 at 10 ft downstream. This indicates good flow quality in the test section. These kinds of prediction about the flow quality in various sections of the new Altitude Wind Tunnel will be verified in 1/10th-scale testing.

Pneumatic Deicers for Helicopter Rotors

NASA Lewis, the U.S. Army, and the B.F. Goodrich Company (BFG) joined in a cooperative effort to develop a prototype pneumatic deicing system for use on a helicopter rotor. NASA Lewis and BFG conducted a test development program in the Lewis Icing Research Tunnel that proved the feasibility of pneumatic boot deicing concepts for helicopter rotor systems. To test the concept in flight, NASA requested the assistance of the U.S. Army. From 1981 to 1984, the Army conducted feasibility flight tests of the system on a UH-1H helicopter. The evaluation included structural loads surveys, performance and

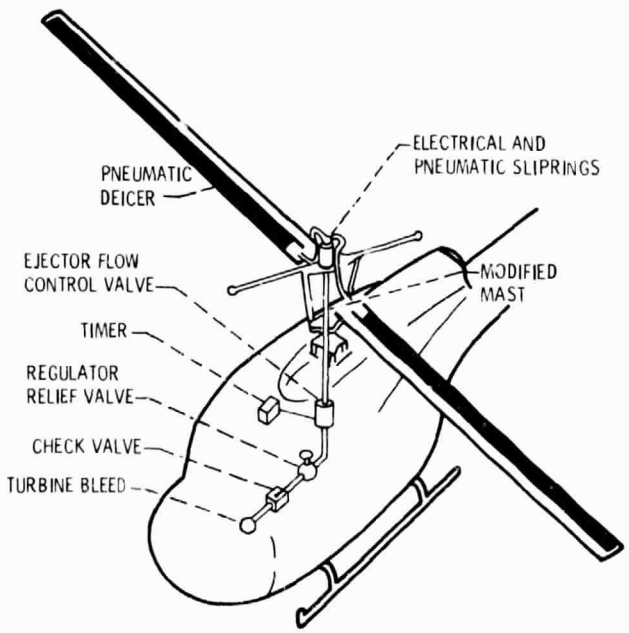

Pneumatic deicer system components

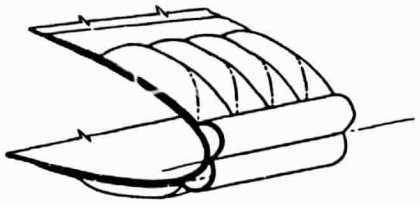

Typical cross section of installed deicer (inflated)

handling tests, rain erosion tests, artificial icing flight tests at the hover spray rig in Ottawa, Canada, and behind the Army's helicopter icing spray system, and limited flight tests in natural icing. Over the development period the prototype system was modified and improved. The current prototype pneumatic deicer system has demonstrated a satisfactory deicing capability in both artificial and natural icing. It is light in weight, low in power consumption, and has acceptable penalties in performance and handling qualities. Pneumatic deicers for helicopter rotors offer an attractive, low-cost, mechanically simple alternative to electrothermal deicers, which are the only systems now in use on helicopters.

Electromagnetic-Impulse Deicing System

Lewis has sponsored a program to develop the electromagnetic-impulse deicing (EIDI) system. The program has included basic analyses, laboratory tests, icing tunnel tests, and flight tests. During the past 2 yr the EIDI system has been tested and refined and has proved to be a low-energy, reliable deicing system. Results show that the EIDI system could have wide application among general aviation and transport aircraft, and possibly even on helicopters. An interaction of magnetic fields and the eddy currents creates an impulsive force on the skin of several hundred pounds for less than a millisecond. A small-amplitude, high-acceleration movement of the skin acts to shatter, debond, and expel the ice.

Among the advantages of the EIDI system are extremely low power requirements—about the same as the aircraft's landing lights; elimination of ducting and engine hot gas bleed requirements

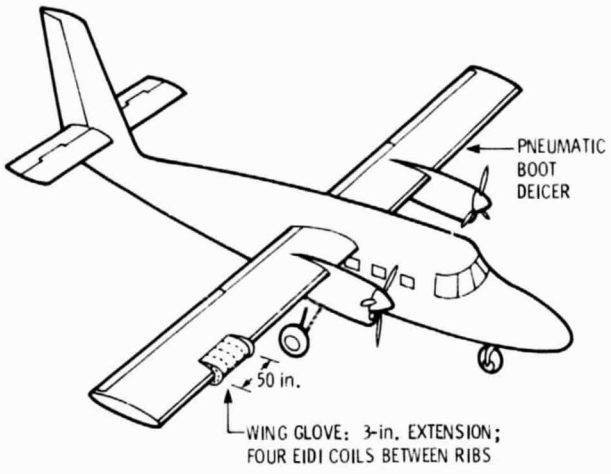

Electromagnetic-impulse deicing flight test

(attractive for tomorrow's advanced turboprop and high-bypass-ratio engines); no aerodynamic penalty, such as with pneumatic boot systems; weights comparable to or less than currently used ice protection systems; and potentially minimal maintenance because there are no moving parts.

A cooperative approach among NASA, university, and aircraft and components manufacturers was chosen for the EIDI program so that the technology gained from the research could be quickly transferred to U.S. aircraft manufacturers. The program is managed by Wichita State University, and a consortium of eight participating industries was formed to represent the whole range of civil aircraft. Consortium members include Beech Aircraft Co., Cessna-Pawnee Division, Gates Learjet Corporation, Cessna-Wallace Division, LearFan Ltd., Boeing Commerical Aircraft Co., McDonnell Douglas Co., Simmonds-Precision, and Rohr Industries.

Large-Scale Advanced Turboprop Systems

New technology is being developed for application to highly loaded, multibladed propellers for use at Mach 0.65 to 0.85. Old-technology propellers are fuel efficient at speeds to Mach 0.6 but suffer intolerable compressibility losses in the higher speed range being explored with advanced blades. Studies show that transport aircraft powered by advanced turboprop engines may use 15 to 30 percent less fuel than advanced turbofan engines (50 to 60 percent less than today's turbofan fleet). Computer codes have been developed jointly by Lewis and Hamilton Standard Division of United Technologies to analyze the structural, aeroelastic, and stability characteristics of these advanced thin, swept blades, which use spar/shell construction. Large-scale verification of this design methodology is required since it is physically impossible to achieve complete structural verification at model scale because of minimum gauge thickness requirements of the blade outer shell. Large-scale (9-ft diam) advanced eight-blade propellers are being built by Hamilton Standard to verify these analytical codes and design techniques at static as well as at simulated flight conditions under the Lewis-sponsored large-scale advanced propeller (LAP) contract. Static rotor tests will begin in 1985.

An uncertainty that must be resolved in the design of these advanced propellers relates to the blade stresses that should be allowed for operation in a nonuniform flow field, such as that caused by the proximity of the engine inlet or a swept wing operating at some angle of attack. Therefore, in August 1984, Lewis awarded a contract to Lockheed-Georgia to mount an advanced propeller and related propulsion system elements on one wing of a Gulfstream GII airplane in order to validate the structural integrity of the propfan design in a real flow-field environment over the entire aircraft flight envelope.

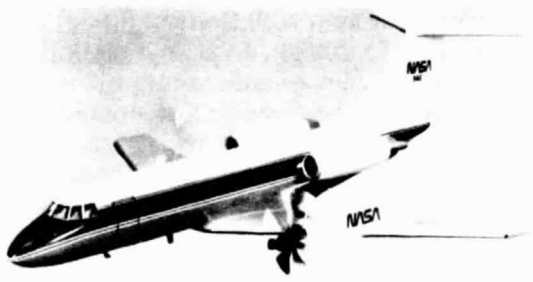

Gulfstream GII testing propfan

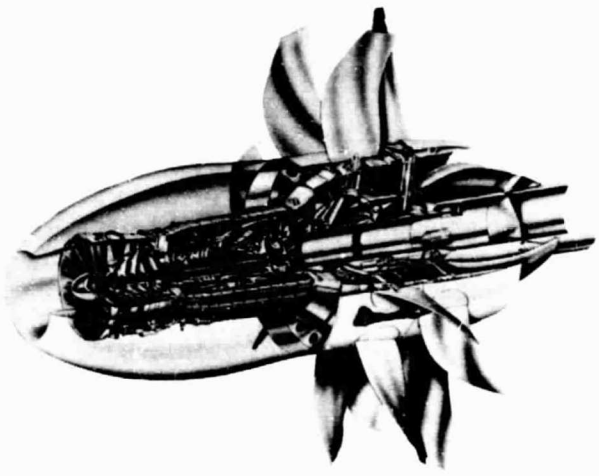

GE unducted fan engine

Other design studies have been made of advanced counterrotation propellers. These propellers can eliminate the swirl, or nonaxial, component of the propeller discharge velocity that is characteristic of single-rotation propellers. This will result in higher propulsive efficiency and thus even lower fuel consumption at a given thrust. Model counterrotation propellers are being tested to evaluate their aerodynamic and acoustic characteristics. Large-scale designs are being synthesized with the aide of NASA-industry-developed aeroelastic computer analysis codes and results from a series of model tests of blade assemblies of various configurations. Because these aeroelastic analytical codes can be verified only with large-scale testing, Lewis entered into a cost-sharing contract with General Electric in February 1984 to design, build, and ground test a unique gearless pusher counterrotation unducted fan (UDF) propulsion system. This concept will also provide an initial assessment of the feasibility of eliminating the gearbox component of the turboprop propulsion system. Existing turboprop gearboxes tend to be heavy and require rather frequent maintenance. Ground static tests of this unique propulsion system will begin in 1985.

In-Flight Noise Measurement for Far-Field Counterrotation Turboprop

Counterrotation turboprops offer the promise of an 8 percent efficiency gain over conventional single-rotation turboprops. However, because of the complexity of counterrotation turboprops, few such systems exist and consequently little noise data on them has been obtained. Although the next generation of counterrotation turboprops will operate at higher rotation and flight Mach numbers, noise data on an existing lower speed model can serve as a starting point for estimating noise of advanced designs. The Fairey Gannet, a 1950's design British military aircraft, employs a fuselage-mounted counterrotation turboprop with four blades in each propeller assembly. This aircraft can maintain level flight with either the forward or aft propeller feathered. The Hamilton Standard Division of United Technologies has acquired one of the last two flyable Gannets and is using the aircraft to study noise generation from the counterrotation turboprop. The aircraft is fitted with an under-wing-mounted microphone boom for near-field noise measurements.

The Lewis Learjet was fitted with wingtip and fuselage nose microphones and flown alongside the Hamilton Standard Gannet to obtain sideline

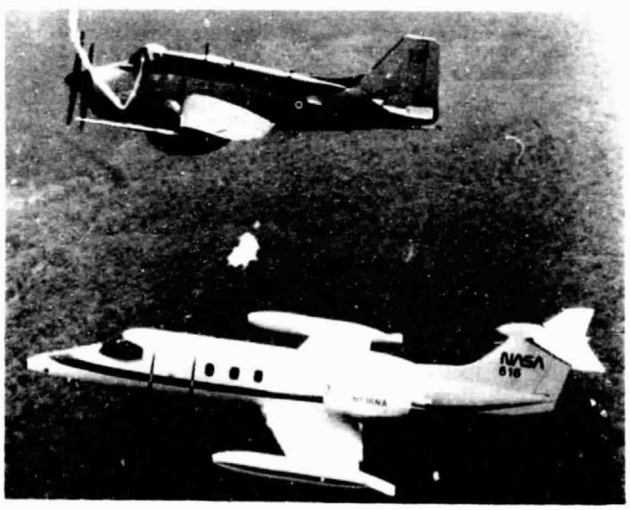

Fairey Gannet and Learjet in flight

noise data at several aircraft separations. Initial analysis of the data has confirmed the presence of circumferential maxima and minima in the sound field. This had been noted in early small-scale, static propeller experiments. These data should prove useful in developing and validating the analytical models of counterrotation turboprop noise required for design studies.

Propeller Pitch-Change Mechanism for Advanced Turboprop Aircraft

Propeller pitch-change mechanism requirements envisioned for advanced turboprop aircraft are significantly more demanding than those for previous systems. Because of the large size of the engine and the blade, blade-pitch-twisting moment torque is of the same magnitude as the main-reduction-gearbox output torque, and blade positional accuracy as well as system reliability are at a greater premium than before. The conceptual design of an innovative pitch-change mechanism that incorporates a high-ratio traction drive together with a high-speed electric alternator/motor drive module has been performed by the General Electric Company under a Lewis contract. This mechanism features a fiber optic data link (coupling), which passes control signal information from the cockpit to the autonomous digital controller mounted aboard the rotating spinner. Mechanical power is shipped across the rotating interface through a shaft connected to the main gearbox. This eliminates the need for electrical sliprings and hydraulic seals, normally high-maintenance items. The high-stiffness, low-hysteresis traction drive coupled to the digitally controlled motor will provide accurate control of blade position. High blade-position accuracy is needed to synchrophase multiple engines and thus minimize the "beating" noise of several propellers.

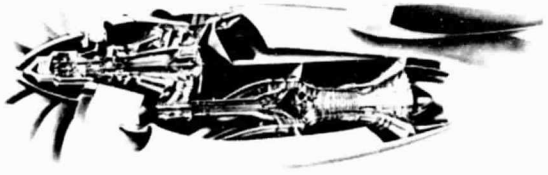

NASA/GE advanced propfan engine technology propulsion system

Measurement of Installation Effects on Turboprop Noise

One of the constraints on using fuel-efficient turboprop propulsion systems is that propeller noise must be limited to acceptable levels in the aircraft cabin and in the community. Knowledge of the propeller source levels is the starting point for quiet cabin design and community projections. Although considerable experimental work has been done on measuring isolated propeller noise in uniform flows, relatively little acoustic information is available for advanced propellers installed on a wing. Theory predicts an

Advanced turboprop and wing in wind tunnel

asymmetric noise field for the propeller operating in the nonuniform flow field associated with the circulation about a wing.

Installation noise experiments were conducted in the Lewis 8- by 6-Foot Wind Tunnel on a 2-ft-diameter model of an advanced turboprop. A wing segment, which spanned the tunnel, was positioned at varying downstream distances to change the degree of flow nonuniformity at the propeller. In addition to microphone measurements to characterize the acoustic field, miniature pressure transducers on the blade surfaces measured the unsteady surface pressures produced as the blades swept through the nonuniform flow field ahead of the wing. As predicted, higher noise levels were produced in the plane of the wing on the side where the blades approach the wing from above. Higher noise levels at forward angles were also observed.

Advanced-Technology Helicopter Transmission

A new helicopter transmission has been built using advanced technology developed at Lewis. Power density has been improved from 2.70 hp/lb to 3.85 hp/lb. Power capacity has been upgraded from 317 hp to 500 hp for the same envelope size and an additional 20 lb weight. Overall transmission efficiency has been improved from 98.5 percent to 98.6 percent. The transmission, designed and built by Bell Helicopter, is the same size as that used in the U.S. Army's OH-58 helicopter. Some of the technology has been incorporated in the Army's Advanced Helicopter Improvement Program (AHIP). Bell also sees other applications for the technology demonstrated in the advanced-technology helicopter transmission.

Advanced technology provided by Lewis gear research engineers includes vacuum-induction-melt-vacuum-arc-remelt steel for bearings and gears, shot-peened gears for improved strength and life, and high-contact-ratio planetary gears for reduced noise, vibration, and tooth loads. NASA research has provided guidance for improved methods of spline, bearing, and gear lubrication and cooling. The bevel gear design was not changed, but the mounting system was designed to carry heavier loads.

Low-Speed STOL Augmentor Ejector Test

Using an air ejector in a short-takeoff-and-landing (STOL) aircraft can augment vertical thrust while minimizing ground erosion and inlet reingestion. Thrust augmentation is provided by a high-pressure air jet that induces extra airflow into the propulsive stream. Such an ejector is incorporated into the General Dynamics E-7 advanced STOL aircraft concept. A 30-percent scale model of this concept was tested in the Lewis 9- by 15-Foot Low Speed Wind Tunnel. Ejector performance was determined over a range of ejector flow conditions and model angles of attack and yaw at low forward velocities simulating STOL and vertical-takeoff-and-landing (VTOL) operating conditions. The ejector performance met the preliminary aircraft design requirements and no operational problems were encountered. This test validates the ejector concept and thus makes it attractive for use in STOL and V/STOL aircraft. The model was later tested in the NASA Langley 4- by 7-Meter Wind Tunnel to study the configuration aerodynamics.

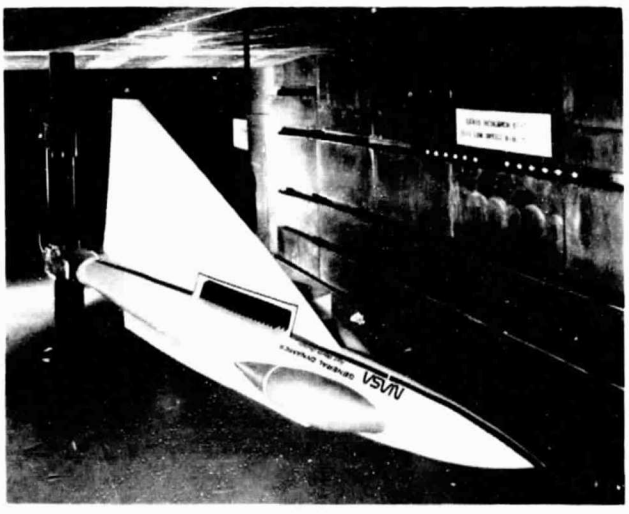

General Dynamics E-7 in wind tunnel

Title	Lewis contact	Phone number, (216) 433-4000, extension—	Headquarters program office
Three-Component Velocity Measurements Using Fabry-Perot Interferometer	Richard G. Seasholtz	353	OAST
Formulation of Blade-Flutter Spectral Analyses in Stationary Reference Frame	Anatole P. Kurkov	5242	OAST
Laser Speckle Photography for High-Temperature Strain Measurements	Frank G. Pollack	356	OAST
Fiber Optic Combustor Viewing System	Frank G. Pollack	356	OAST
Application of Infrared Photography to Turbine Vane Temperature Mapping	Frank G. Pollack Orlando W. Uguccini	356 354	OAST
Flow Measurements in Internal Combustion Engines	Harold J. Schock	5236	OAST
Computer Program for Rotordynamic Analysis	David F. Fleming	6975	OAST
AESOP—A Program for Computer-Aided Design of Linear Multivariable Systems	Bruce Lehtinen	474	OAST
Real-Time Multiprocessor Simulator	Dale J. Arpasi	5129	OAST
Influence of Stator Endwall Contouring on Performance of Small Turbines	Jeffrey E. Haas	6169	OAST
Variable-Area Radial Turbine	Richard J. Roelke	5212	OAST
Turbine Bypass Engine	Leo C. Franciscus	6183	OAST
Topping-Cycle Engine	George E. Turney	5124	OAST
Low-Speed Aeroacoustic Performance of a Supersonic Axisymmetric Mixed-Compression Inlet	Charles J. Trefny	5272	OAST
Buoyancy Effect on Laminar Heat Transfer in a Rotating Tube	Robert Siegel	6847	OAST
Experiments and Modeling of Dilution Jet Flow Fields	James D. Holdeman	5307	OAST
Compressor Blade Row Interactions	Michael D. Hathaway	6846	OAST
Model Equation for Simulating Flows in Multistage Turbomachinery	John J. Adamczyk	5518	OAST
Turbulent Solutions of the Equations of Fluid Motion	Robert G. Deissler	351	OAST
Analytical Modeling of Circuit Aerodynamics in New Altitude Wind Tunnel	Charles E. Towne	5520	OAST
Pneumatic Deicers for Helicopter Rotors	John J. Reinmann	5542	OAST
Electromagnetic-Impulse Deicing System	John J. Reinmann	5542	OAST
Large-Scale Advanced Turboprop Systems	Gilbert K. Sievers	317	OAST
In-Flight Noise Measurement for Far-Field Counterrotation Turboprop	John F. Groeneweg	5372	OAST
Propeller Pitch-Change Mechanism for Advanced Turboprop Aircraft	Bruce M. Steinetz Stuart H. Loewenthal	6101 6839	OAST
Measurement of Installation Effects on Turboprop Noise	John F. Groeneweg	5372	OAST
Advanced-Technology Helicopter Transmission	Dennis P. Townsend	5258	OAST
Low-Speed STOL Augmentor Ejector Test	Laurence W. Gertsma	6668	OAST

Space Communications

Spectrum/Orbit Utilization Program for Geostationary Satellites

Current and projected demands on the use of the geostationary orbit/spectrum resource require an analytic tool for determining the interferences among operating and planned communications systems. Before a satellite system is developed, a detailed analysis must be performed to determine the expected interference environment during operations. Such calculations determine the permitted spacing between satellites and the limits on the capacity of a particular orbit/spectrum segment. The spectrum/orbit utilization program (SOUP) is an analytic computer program that has been developed for this purpose. The major computed outputs are the carrier-to-interference ratios at specified Earth station receiver sites.

The program, as presently configured, can handle 300 downlink service areas and 300 uplink service areas. Each service area pair is associated with a satellite in geostationary orbit. There can be as many as 1600 uplink transmitter sites and 4500 Earth station receiving sites. Downlink and uplink interferences are mathematically combined, and the total interference is compared with a given requirement that varies with modulation type, grade of service, and other parameters. Rain attenuation and other propagation effects can be taken into account.

The SOUP program was developed under contract with ORI, Inc., over a period of years and was used as the official analysis program at the 1983 Regional Administrative Radio Conference (RARC). Currently the program is being used at Lewis to evaluate alternative arrangements of satellites in the fixed satellite service (Domsats).

20-GHz, 75-W Traveling-Wave Tube

A multimode, helix type of traveling-wave tube (TWT) that can be used in space applications for geosynchronous communications satellites at frequencies of 20 GHz has been successfully developed. The Hughes Aircraft Company, under contract to Lewis, has fabricated and tested four complete TWT units. This TWT is one of the first high-power units built and demonstrated for application in the 20-GHz frequency band that is capable of space application. Saturated radiofrequency output power levels to 80 W and a power gain of 40 dB from 18.0 to 20.5 GHz have been demonstrated. The TWT design is currently being implemented at the 40-W level for use in the 20-GHz downlink transmitter of the NASA 30/20-GHz Advanced Communications Technology Satellite (ACTS), which is scheduled for launch in 1989.

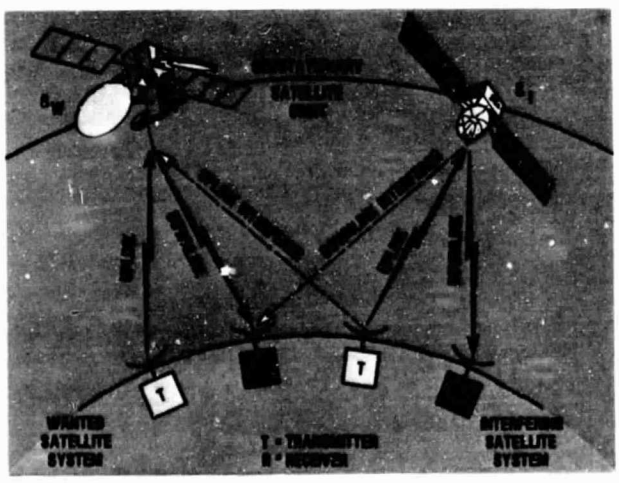

Simplified model of SOUP

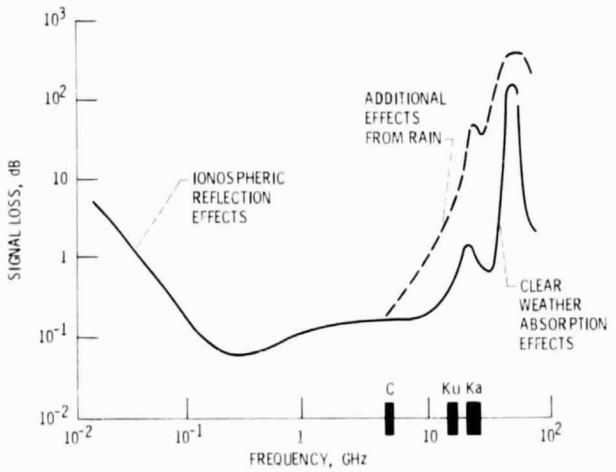

Radio signal attenuation

The TWT is an electronic device for amplifying radiofrequency signals that propagate along a tungsten-ribbon helix that surrounds a highly focused electron beam. Through a complex electric-magnetic interaction process the velocity of the electrons in the electron beam is precisely synchronized and modulated to produce an energy exchange between the electron beam and the rf signal. By careful design the rf signal power in a TWT can be increased as much as 100 000 times.

A major disadvantage that is encountered in the 30/20-GHz frequency band is signal loss due to atmospheric moisture, which can significantly degrade the quality of the received signal. Heavy rain in particular can severely attenuate the downlink signal and interfere with or even interrupt the service unless the rf power signal is increased. To compensate for atmospheric losses and achieve uninterrupted service, the TWT permits the rf output power to be controlled over the range 5 to 50 V by varying the anode voltage.

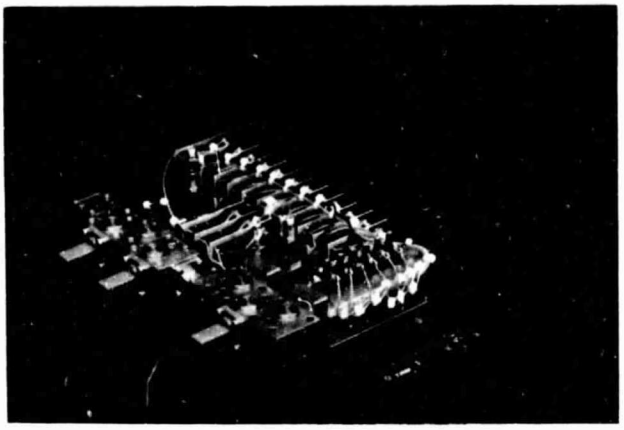

IMPATT transmitter

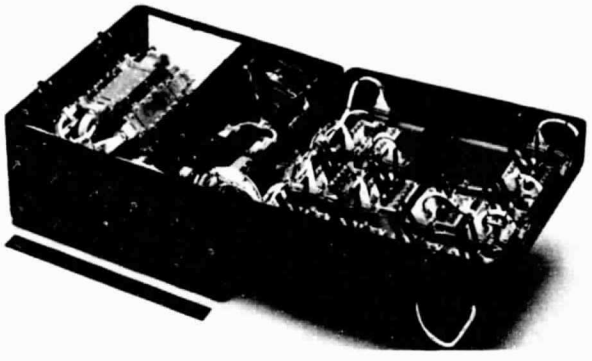

FET transmitter

Solid-State Transmitters for Advanced Communications Satellites

Because they may be more reliable, solid-state devices are a potentially attractive replacement for traveling-wave tubes. Single solid-state devices are not competitive with traveling-wave tubes with respect to power output or high-power efficiency. However, they appear to offer, in conjunction with either circuit or spatial power-combining techniques, a useful alternative to tubes at power levels to about 20 W.

Lewis is investigating two types of solid-state devices for transmitter applications: the gallium arsenide field effect transmitter (GaAs FET) and the impact avalanche and transit time (IMPATT) diode. Each type has distinct advantages and disadvantages. As a three-terminal device the FET offers increased stability, linear amplification, good input-output isolation, and greater bandwidth. The IMPATT diode, on the other hand, as a negative-resistance device, is capable of higher output power and higher efficiency in the microwave region. Most IMPATT diode work has concentrated on operation in an injection-locked mode, although recent work has shown that nearly equivalent power and efficiency can be achieved in a stable-amplifier mode.

Considerable progress has been made toward developing reliable, low-power GaAs FET transmitters for potential application on advanced communications satellites. Two versions of such a transmitter have been built under Lewis sponsorship by TRW and Texas Instruments. Their key features are radiofrequency output powers of 8.0 and 8.95 W and bandwidths of 1.2

and 1.7 GHz, respectively. The amplifiers achieve the required power capability by using appropriate circuitry to combine the power outputs of 8 and 16 parallel modules, respectively.

Lewis has also sponsored two contracts for IMPATT development. TRW has developed a transmitter with 15.5-W output and a 0.1-GHz bandwidth in the injection-locked mode. The contract to LNR Communications, Inc., called for development of IMPATT devices and the design only of a 20-W transmitter. LNR successfully developed 2.0-W diodes with better than 20 percent efficiency. The design produced under this contract has been used in demonstrating 20 W of output power over a bandwidth greater than 1 GHz.

Microwave Monolithic Integrated Circuit Transmit Module

The expanding utilization of existing frequency and orbital slot resources puts increasing pressure on designers of communications satellites to maximize operating efficiency while minimizing cost. Studies indicate that a major factor in achieving these goals will be the use of multiple scanning beam antennas. For this application gallium arsenide microwave monolithic integrated circuits (MMIC) offer substantial advantages in cost, weight, efficiency, and switching speed. Since entire microwave circuit functions can be implemented on a single chip, the resulting circuit can be fabricated inexpensively in large quantities with little or no performance variation. Lewis is presently pursuing a number of MMIC circuit developments at 20- and 30-GHz frequency ranges.

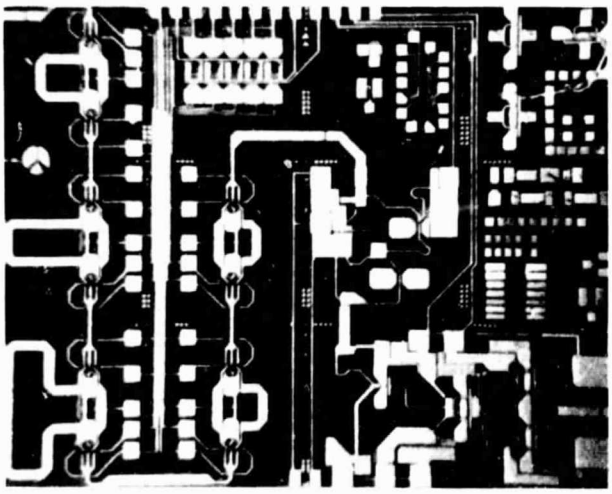

20-GHz monolithic transmit module

Under a contract from Lewis, Rockwell has developed the first fully monolithic transmit module suitable for implementation into a 20-GHz phase array transmit antenna system. The module has 125-mW output power, 15-dB gain, and 32-step phase control from 0° to 180° and operates in the frequency band 17.7 to 20.2 GHz.

Channel Model Simulation Program

To optimize the performance of a satellite communications transponder, various alternative hardware configurations must be examined and compared. Doing this with actual hardware is extremely costly and time consuming. A less costly and faster method is to numerically simulate the transponder. Components are modeled with relatively simple algorithms, and changes to hardware can be evaluated with slight changes to these algorithms. The accuracy of the simulation is limited only by the computational resources.

Stanford Telecommunications Incorporated, under contract to Lewis, has modified and extended an existing software simulator, the Channel Model Simulation Program (CMSP), to allow for a complete simulation of NASA's Advanced Communications Technology Satellite (ACTS). The new simulator includes features for numerous modulation methods, channel filtering, nonlinear components, satellite baseband processing, error-correcting coding and decoding, and carrier/clock acquisition and tracking. The outputs include power spectra at requested locations, bit error rate performance, and acquisition performance.

The University of Toledo, under a grant from Lewis, has used this simulator to predict the performance of a hypothetical transponder consisting of the proof-of-concept components now being completed as part of the ACTS program. They have demonstrated that very complex satellite transponders can readily be simulated and that the accuracy of the simulation is sufficient to determine correction measures needed to optimize satellite communications channels.

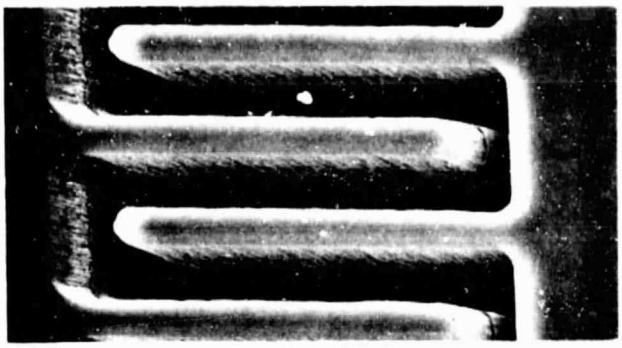

Interdigital electrode pattern

Submillimeter-Wave Backward-Wave Oscillator

High-frequency oscillators are needed by astronomers as local oscillators to perform spectroscopy in submillimeter-wave observatories. Under a grant from Lewis, the University of Utah is designing and fabricating a submillimeter-wave backward-wave oscillator (BWO) that will be suitable as a local oscillator. The initial attempt is to produce a BWO that operates near 600 GHz.

The BWO uses an interdigital line for a slow-wave structure. The line is etched into a diamond substrate by a process developed at Lincoln Laboratories. Cold tests of a scaled interdigital structure etched into a dielectric material predict that this structure will produce electromagnetic radiation over the frequency range 400 to 660 GHz. Testing of an oscillator will begin shortly. If successful, this program will result in the production of wide-band, high-frequency local oscillators necessary for astronomical observations in the submillimeter-wave frequency range.

30-GHz Power Amplifier

Future Ka band satellite ground terminals must be small, low-data-rate terminals with highly reliable, low-cost 30-GHz uplink amplifiers. Under contract to Lewis, TRW has designed, fabricated, and tested a solid-state 20-W output device. The design includes the use of double-drift, silicon impact avalanche and transit time (IMPATT) diodes in a waveguide resonator power-combining circuit. The transmitter may be used in either a time-division multiple access (TDMA) or frequency-division multiple access (FDMA) mode. The radiofrequency bandwidth is greater than 250 MHz, thereby permitting low to medium (110 megabits/s) data rates.

Title	Lewis contact	Phone number, (216) 433-4000, extension—	Headquarters program office
Spectrum/Orbit Utilization Program for Geostationary Satellites	Edward F. Miller	240	OSSA
20-GHz, 75-W Traveling-Wave Tube	Ernie W. Spisz	713	OSSA
Solid-State Transmitters for Advanced Communications Satellites	Gerald J. Chomos	5279	OSSA
Microwave Monolithic Integrated Circuit Transmit Module	Thomas J. Kascak	5560	OAST
Channel Model Simulation Program	Grady H. Stevens	226	OSSA
Submillimeter-Wave Backward-Wave Oscillator	Norbert Stankiewicz	5562	OAST
30-GHz Power Amplifier	Dale E. Pope	792	OSSA

Space Technology

Space Propulsion

Radiation Exposure in LEO/GEO Transfers

Presently geosynchronous equatorial orbit (GEO) satellites are carried to low Earth orbit (LEO) by the shuttle, deployed, and then transferred to GEO by an upper stage or orbit transfer vehicle. Because proposed large, lightweight spacecraft are structurally sensitive, a multiburn, low-thrust trajectory was designed to satisfy the acceleration limits with negligible propellant penalties. However, the multiburn transfer results in longer trip times, which increase radiation exposure.

By using the multi-perigee-burn strategy, trajectories were defined for one-, two-, four- and eight-burn LEO/GEO transfers. The time-position history for the trajectories and the latest proton and electron radiation environment models were then correlated to determine dose rates and total dose as a function of radiation type. Radiation exposures were calculated to establish shielding requirements for astronauts and electronics. Results indicate that astronauts could safely perform LEO/GEO orbit transfers if shielded by the moderate protection now used in the shuttle. Transfer times vary from about 5 hr for one burn to about 28 hr for eight burns.

The analytical technique developed can be used by spacecraft designers to define the moderate shielding requirements for both crew and electronics. Considerable flexibility has now been given to the mission planners in terms of alternative mission strategies and options for system reliability.

High-Pressure-Turbopump Impeller Seal

The high-pressure fuel turbopump for the space shuttle main engine has shrouded centrifugal impellers with integral labyrinth seals on the forward outer diameters. The rotating knife-edges are a titanium alloy (Ti-5Al-2.5Sn) and the stationary seal rings are aluminum. This combination permits minimum clearance since the soft aluminum can be easily worn by the harder titanium when rubbing occurs. Seal clearance is critical to the turbopump's efficiency—a 0.005-in. increase over the three stages can cause a 2 percent loss due to backflow of high-pressure hydrogen. Cracks in the knife-edges have been observed in service. Clearance penalties have resulted from direct rotor (knife-edge) wear and from "blobs" of material transferred from the static seal to the rotor.

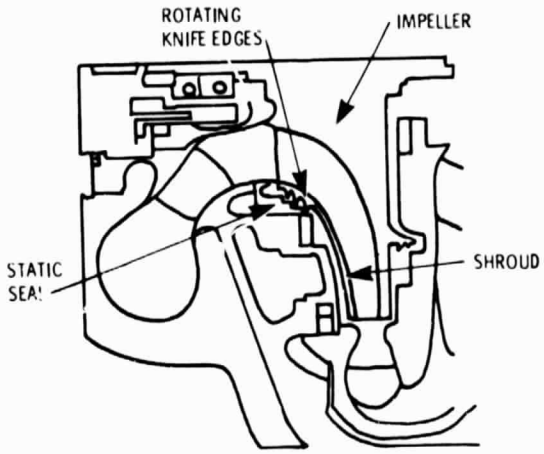

High-pressure fuel turbopump showing impeller seal detail

In an effort to improve the durability and efficiency of the impeller shroud seals, an experimental evaluation was conducted. It was concluded that the knife-edge cracks are caused by cyclic thermal stresses resulting from rub-induced thermal loads. Furthermore an alternative seal combination consisting of uncoated titanium alloy knife-edges and plasma-sprayed aluminum-graphite can eliminate both the wear and the material transfer. With this new combination the static portion is cleanly grooved by the rotating knife-edges and produces no detectable frictional heating of the impeller. Rub forces are also very low. Thus the impeller seal configuration of titanium alloy on the rotor and aluminum-graphite on the housing can eliminate or greatly reduce clearance changes and seal degradation. This

configuration could remove this seal as a life-limiting factor in the space shuttle main engine.

Large Vaporizers for Mercury Ion Thrusters

A key technology area in the design of ion thrusters is the vaporizer assembly, which serves as a flow control device to meter mercury propellant to the thruster and cathodes. The present 30-cm-diameter thruster requires a propellant flow through the main vaporizer that will produce a screen current of 2 A. This is equivalent to 14.96 g/hr. Higher performance thrusters require greater propellant flow. Propellant flow can be increased either by increasing the area or by decreasing the density of the porous tungsten. However, the density is already at the minimum to satisfy other requirements and the electron beam welding of the porous tungsten to the holder is limited by size. Therefore a fabrication technique was needed that would allow large, porous tungsten vaporizers to be manufactured.

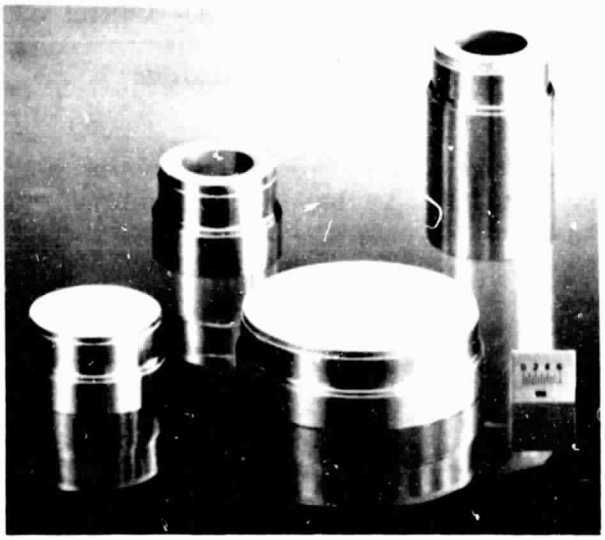

Large vaporizers for mercury ion thrusters

A molybdenum/ruthenium braze was used to attach the porous tungsten to the holder because it is compatible with mercury and does not wick into the porous tungsten during brazing. This brazing technique was used to make both disk- and cylinder-shaped vaporizers. The diameter of vaporizers that can be manufactured is no longer the limiting factor in the design of high-performance mercury ion thrusters. Vaporizer-to-tube assemblies of all sizes can now be mass produced.

Flow Analysis of Turbine Exhaust Duct

The space shuttle main engine (SSME) is a high-performance, liquid-propellant (hydrogen-oxygen) rocket engine. The engine uses a staged-combustion power cycle. Hydrogen-rich gas powers the high-pressure turbopumps and, along with additional oxidizer and fuel, is routed into the main combustion chamber at a high mixture ratio and high pressure. Flow separation in the turbine exhaust ducting, which carries approximately 75 percent of the fuel to the main injector, can create a pressure drop between the turbopump and the main combustion chamber. This would result in reduced engine performance. In addition, flow separation creates disturbances that can propagate into the main injector-post regions, thereby contributing to injector-post failures.

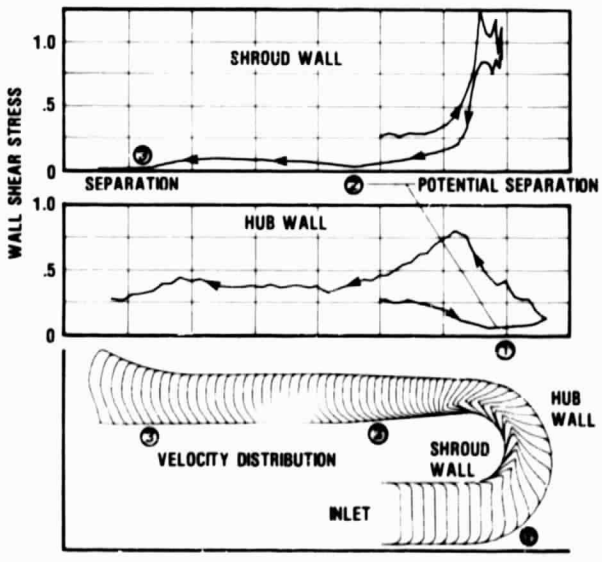

Flow analysis of SSME turnaround duct

Flow within the SSME exhaust duct was examined analytically to determine the potential for separation. An axisymmetric/turbulent viscous computation was performed using a Lewis fluid dynamics computer code. The computation was based on the turbine exit design conditions. The results may explain some performance loss in the existing duct design. Examination of modified turnaround ducting geometries using available analytical tools may identify configurations with lower pressure drops and better performance.

Measuring Stress in Thin Films

Thin films have many useful applications. However, in ion thrusters and other plasma devices, thin-film formation may be life limiting. The stress in a thin film is an important factor in its adhesion and in its behavior under temperature variation. If the stress in the film becomes large enough to exceed the adhesion bond strength of the film-substrate interface, the film will buckle and eventually peel off. Present stress-measuring techniques (such as Newton rings and surface analyzers) are rather complicated and time consuming. A new, much quicker method of stress measurement in thin films has been developed. This can significantly facilitate the study of film adherence to substrates.

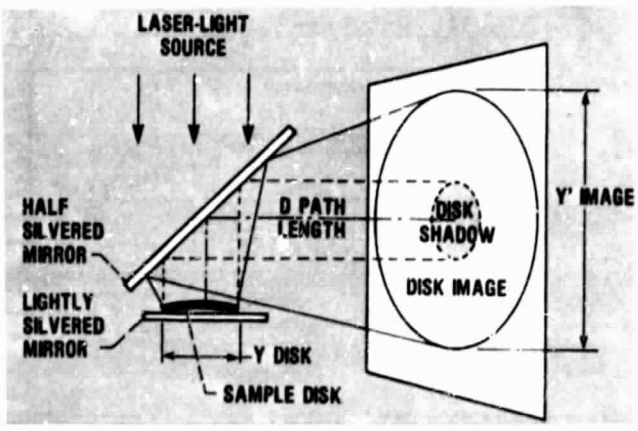

Measuring stress in thin films

Geometrical optics were applied to project the image of a thin film by a laser light beam onto a screen. The measurement of the focal length of the "spherical mirror" will closely approximate the radius of curvature of the thin film; from this measurement the stress of the film can be determined. The new method has been applied to measuring stress in thin films formed in ion thrusters. The new technique provides quicker and more accurate stress measurements than standard methods.

Simplified Power Processor for Ion Thrusters

Historically, electric thruster systems have required a power processor to provide highly regulated currents and voltages to the thruster and its control unit. Present complex systems have evolved because of the need to satisfy the requirements of many space missions. It has been recently demonstrated under contract to Lewis that power processor requirements can be simplified without sacrificing mission requirements.

A simplified power processor and control unit built and tested by Hughes Research Laboratories has achieved nearly a tenfold reduction in the number of parts at a higher power capacity (600 vs. 165 W). Simplification was attained (1) by reducing the number of supplies by combining their functions, (2) by reducing the thrust accuracy and the regulation requirements, (3) by minimizing the number of operating set points, and (4) by using state-of-the-art power processor technology. Tests with an 8-cm-diameter mercury ion thruster have demonstrated the capability of the simplified power processor to perform as required. The new technology makes ion thruster propulsion systems more competitive and attractive for new missions by improving the reliability and reducing the system weight and cost.

Spacecraft Charge Control

During portions of a geosynchronous spacecraft's orbit, electrons are collected on various satellite surfaces. Electrical discharging due to the buildup of charge on insulating surfaces has been observed often and is believed to be responsible for many operational malfunctions and disruptions. A device capable of efficient control of spacecraft charging would eliminate this area of concern for many types of geosynchronous spacecraft.

Plasma-bridge hollow cathodes have been developed in-house and by contracted efforts at the Hughes Research Laboratories (HRL) as extremely efficient sources of ions and electrons for ion thruster systems. Additionally, unique instruments that monitor spacecraft charging have been developed in-house as part of a joint Air Force-NASA spacecraft-charging program. The Air Force Geophysics Laboratory has contracted with HRL to develop a spacecraft-charging sense and control unit. The unit will use a hollow cathode, operated on xenon, along with the monitoring instruments that evaluate the spacecraft surface potential and transient pulses that result from electric discharges. The hollow cathode will operate in a closed loop with the potential monitors to actively control spacecraft charging and eliminate problems associated with discharging.

Thermal Barrier Coatings for Rocket Thrust Chambers

Reusable rocket thrust chambers that operate at very high chamber pressures encounter an irreversible plastic deformation of the cooling passage wall during each thermal cycle. After numerous thermal cycles, cracks that can lead to failure of the thrust chamber form in the cooling passage wall. A thermal barrier coating, such as zirconium oxide, applied to the thrust chamber cooling passage wall can substantially increase the life of the chamber. The coating reduces the cyclic-induced plastic strain that causes the wall to deform. The normal procedure of applying the ceramic coating is to plasma spray the coating on an already fabricated chamber. It is difficult to obtain a good bond with this technique because the substrate oxidizes during the coating process. The bond is further weakened by the large intrinsic stress that remains in the coating when it cools to room temperature.

Lewis has developed an "inside out" fabrication technique that reduces the oxidation and stress problems. The coating is sprayed onto a mandrel and a copper liner is electrodeposited around the coating. The cooling passages are then machined into the copper liner and the wall is closed out in the conventional manner by electrodeposition. When the mandrel is removed, a smooth zirconium oxide coating is left on the inner wall.

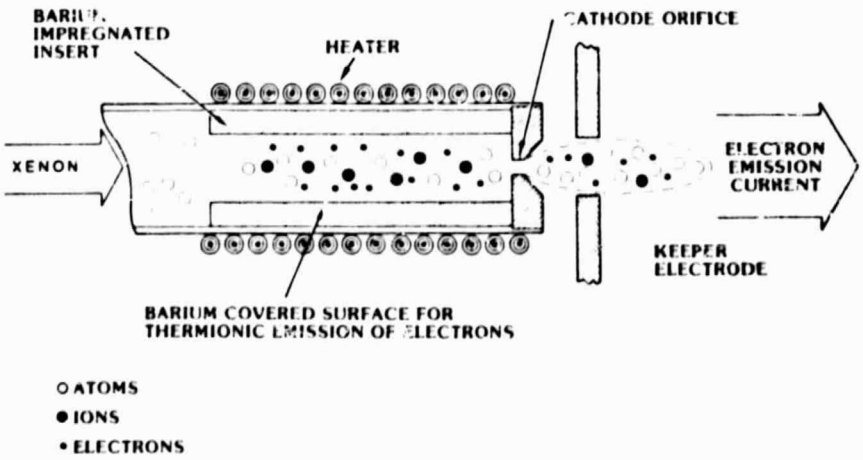

Hollow-cathode technology

Several subscale rocket thrust chambers have been fabricated at Lewis using this technique. Coatings as thin as 0.003 in. have been achieved. The chambers were thermally cycled and the test results compared with results for identical chambers without coatings. On the average, cracks formed in the uncoated chambers after 150 cycles. The coated chambers survived a minimum of 1500 cycles with no cracks in the cooling passage wall and with little or no coating loss in the high-heat-flux region of the throat.

IAPS 9000-hr Ground Test Completed

Present long-life satellites (e.g., communications satellites) are dominated by the hydrazine storage tanks needed for auxiliary propulsion tasks such as north-south stationkeeping. The high specific impulse of electric propulsion can reduce the propellant requirement significantly. On a 10-yr satellite, hundreds of kilograms of propulsion system weight savings can be realized. Benefits increase with larger satellites and longer mission times.

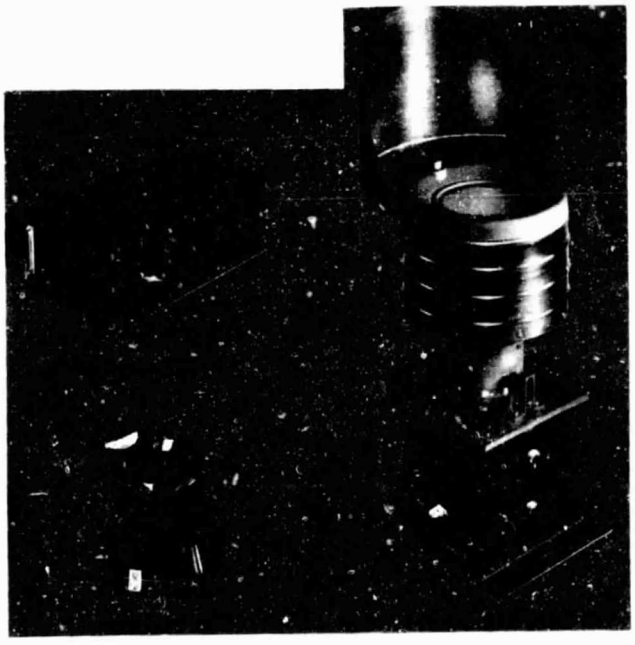

IAPS test components

To meet the thrust requirements of a typical geosynchronous satellite for north-south stationkeeping, an auxiliary electric propulsion system must be capable of 7500 hr of operation with 2500 restarts. A ground test of the critical units representative of the ion auxiliary propulsion system (IAPS) flight hardware has been completed with operation of the ion thruster for 9487 hr in a vacuum environment. In addition, 652 on-off cycles have been completed by the test subsystem, which included a thruster-gimbal-beam shield unit, a power electronics unit, and a propellant tank, valve, and feed unit. These long-term ground tests have shown successful operation for significantly longer times than either the IAPS mission requirements or a typical mission application. The 10 266 hr accumulated by the power electronics unit is the longest test of electric propulsion system electronics.

The unique features of electric propulsion such as high specific impulse, low thrust, and long life have been well known for almost two decades. Operational acceptance has been delayed by a lack of qualified flight hardware. That hardware is now available, it has been qualified, and it is ready for flight test aboard a shuttle-launched Air Force satellite.

Space Power

Advanced Photovoltaic Experiment

The Advanced Photovoltaic Experiment (APEX) was developed by Lewis for flight aboard the long-duration exposure facility (LDEF) to evaluate the effects of long-term space exposure on advanced and conventional solar cells. The LDEF was transported into space by the space shuttle on flight STS-41C, which was launched on April 4, 1984. The LDEF will be retrieved from space by the flight of STS-51D, with a scheduled launch date of March 18, 1985.

Techniques used to correlate cell performance in space with that of ground simulators will be verified by APEX data. Reference cells, including

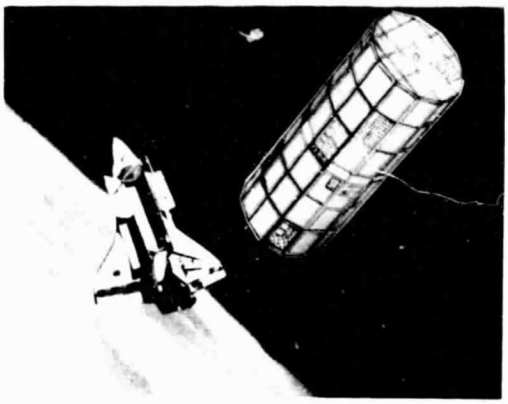

Advanced photovoltaic experiment

some previously measured on balloon, aircraft, and rocket flights, will serve as laboratory standards for accurate predictions of performance in space for other cells and arrays.

The APEX is composed of 152 solar cells plus a radiometer to measure the total solar energy and a digital solar angle sensor to measure the angle of incidence of the direct solar energy. The solar cell performance will be measured before flight, during flight, and again after the experiment is returned to Earth. Data will be obtained daily in flight, recorded on magnetic tape by the APEX data system, and analyzed when the experiment is returned to Earth.

IR-100 High-Voltage, High-Power Remote Power Controllers

A family of seven remote power controllers (RPC's) developed by Lewis was selected by Research & Development Magazine to receive an IR-100 award as one of the 100 best new products of 1984. All the RPC's combine circuit-breaker and remote-switching functions with a microsecond trip point for high overloads. The family uses gate-turnoff (GTO) thyristors and metal oxide surface field effect transistors (MOSFET) as the switching devices. Power ratings span the range from hundreds of watts to 52 kW and current and voltage ratings extend to 100 A and 1200 V. All devices have efficiencies

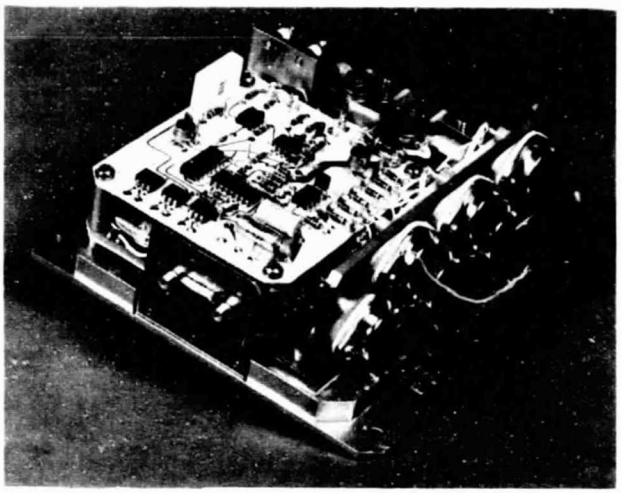

MOSFET type of remote power controller

close to 99 percent and are suitable for a wide variety of applications including spacecraft, aircraft, and industrial.

Advanced-Design Nickel-Hydrogen Cells

As a part of an overall effort to advance the technology of nickel-hydrogen cells and batteries, improved designs for individual pressure vessel (IPV) cells have been conceived and built and are now being life tested. The purpose of this effort is to improve the cycle life at deep depths of discharge. State-of-the-art cells (Air Force/Hughes and Comsat) are adequate for geosynchronous orbit applications, where not many cycles are required over the life of the storage system. However, for the demanding low-Earth-orbit applications, the current cycle life at a deep depth of discharge (2000 to 8000 cycles) is not acceptable.

Two different modifications to existing IPV nickel-hydrogen cell designs have been designed. They differ mainly in the method of oxygen management. New features of these advanced designs that are not incorporated in either the Air Force/Hughes or Comsat design cells are alternative methods of oxygen recombination to aid thermal management and to prevent damage

to the hydrogen electrodes, serrated-edge separators to facilitate gas movement, and an expandable stack to accommodate nickel electrode expansion.

The advanced designs also consider electrolyte management over the life of the cells. They are fully compatible with state-of-the-art cells, which should minimize development cost and time. Boilerplate cells based on each of the designs have been built by a commercial supplier to Lewis' specifications and are being cycle tested to verify design feasibility.

Synthetic Battery Cycling of Sodium-Sulfur Cells

Sodium-sulfur cells and batteries offer potential as high-energy-density systems for aerospace applications. However, the life of the ceramic separator materials must be extended, and an assembled group of cells must be cycled as a battery without an undue amount of control circuitry. In a recent study a 68-cell sodium-sulfur "battery" was modeled with the use of suitable electrical network theory. Cell parameters were assigned to each individual cell on a random basis, but the variability of the resistance and capacity were limited to 5 percent of their nominal values. The battery configuration consists of four cells in parallel and 17 of these parallel sets connected in series. A mainframe computer was used to alternately discharge and charge this grouping of cells. The results showed that a battery in geosynchronous orbit, where the maximum depth of discharge would be 80 percent, would cycle properly for 10 yr. Results also show that cells are least prone to divergence when the maximum number of cells is grouped together in parallel.

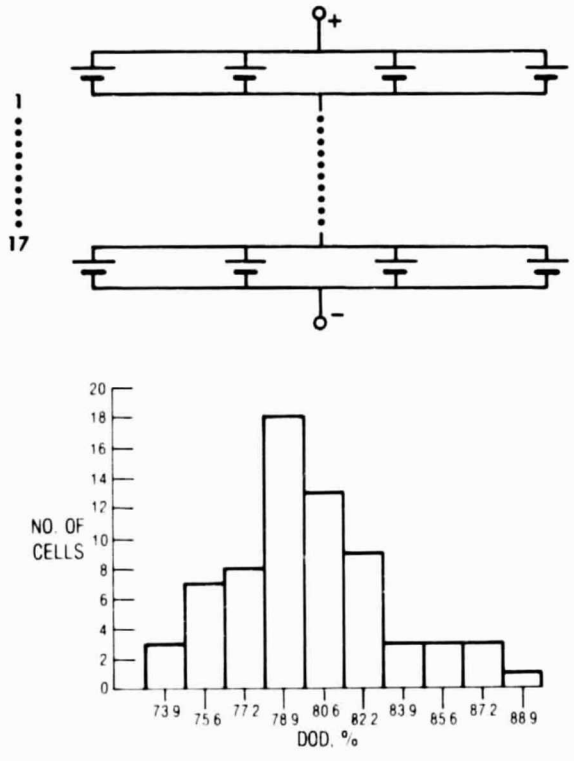

Configuration and depth-of-discharge distribution for sodium-sulfur battery

Advanced Electrocatalysts for Phosphoric Acid Fuel Cell Powerplants

Under a Lewis advanced research contract to develop better electrocatalysts for phosphoric acid fuel cells, Giner, Inc., has developed several improved catalysts that contain an alloy of platinum and one or two other metals. In studies

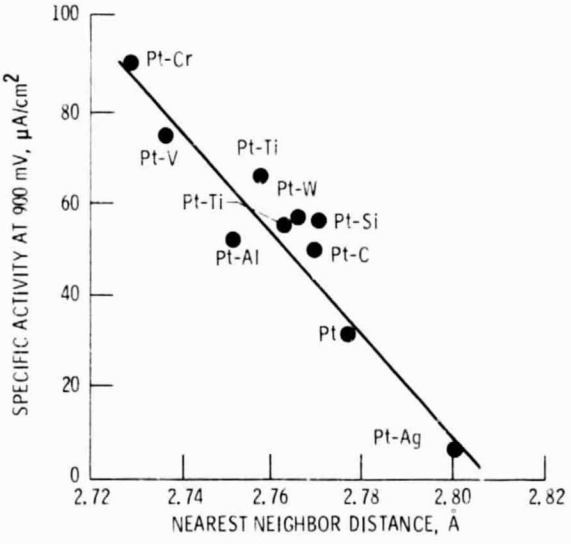

Specific activity for oxygen reduction in platinum alloys

made to understand the reasons for the enhanced activity of supported platinum alloys, a correlation between the oxygen reduction activity and the platinum interatomic spacing was observed. It appears that the magnitude of the change in the platinum-platinum distance is controlled by the alloying metal species and its concentration in the alloy. This correlation provides a valuable guideline for selecting high-activity platinum alloys for use in phosphoric acid fuel cell powerplants.

Simulation of Phosphoric Acid Fuel Cell Powerplants

Under contract to Lewis, Cleveland State University has developed several codes to simulate steady-state and transient operation of the phosphoric acid fuel cell (PAFC) system. One of the steady-state codes has been used to predict the optimal configuration in the design of fuel (hydrogen-rich gas) and oxidant (such as air) flow channels in the fuel cell stack. The resulting U-flow configuration has more uniform current density distribution than the present design. The heat-exchanger-network code is being used to resynthesize energy management in order to optimize facility and operating costs. The newly developed transient model provides understanding of the effects of sudden load changes and load ramping on system performance.

Verification of Electric Utility Fuel-Cell-Stack Technology

Under contract to Lewis, considerable progress has been made in verifying the endurance and performance goals established for the baseline cell configuration of the prototype power section for the 11-MW commercial-feasibility powerplant. A 3.7-ft^2-planar-area, 20-cell short stack has attained 8000 hr of stable operation; a second 3.7-ft^2, 30-cell short stack is still on test after 12 700 hr. The 3.7-ft^2 cell technology was scaled up to 10-ft^2 prototype powerplant size and a successful 1500-hr test was run.

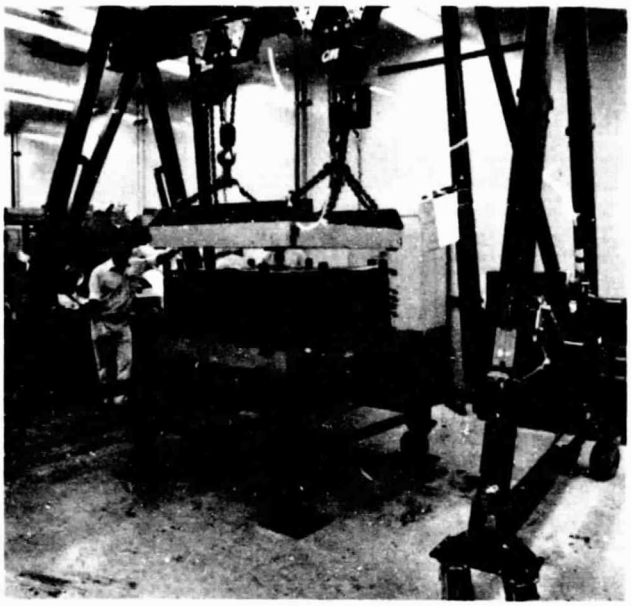

10-ft^2, 30-cell fuel cell short stack

Advanced Alkaline Fuel Cell Technology

A four-cell battery stack containing several advanced-technology features is being endurance tested by United Technologies Corp. The stack contains a platinum-on-carbon anode catalyst, a bonded titanate matrix, and a graphite electrolyte reservoir plate. The anode catalyst has already surpassed 16 500 hr in another endurance test. The matrix has been developed to provide a higher temperature operating capability (250 °F) than the asbestos matrix now used in space shuttle fuel cells. This material has demonstrated better resistance to chemical attack and better voltage stability than asbestos in long-term performance tests at 250 °F. Problems related to its fabrication as a free-standing matrix have been resolved. The graphite electrolyte reservoir plate costs less than the standard sintered-nickel plate and reduces the weight of the cell stack by 47 percent.

Although the components of this stack were developed primarily for long-life, stable performance on a space station, the lightweight,

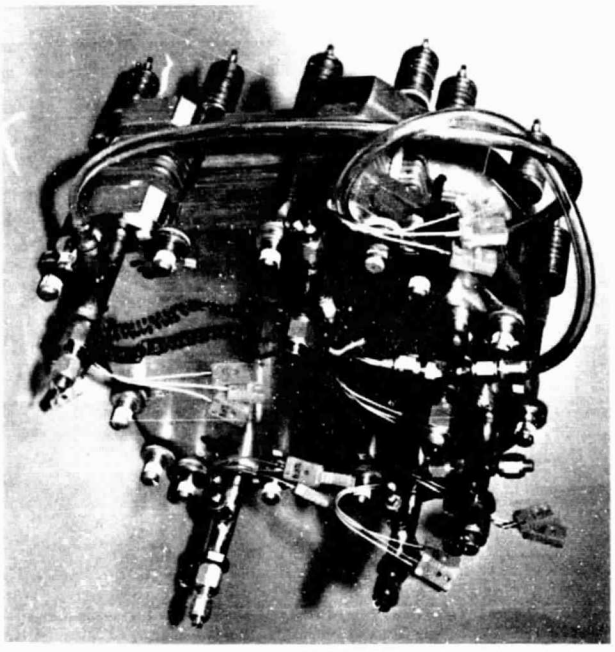

Advanced-technology fuel cell stack

high-temperature capability should also benefit future fuel cell applications, such as the fuel cell for the orbital transfer vehicle.

Ultralightweight Gallium Arsenide Solar Cells

An important aspect of the NASA program in space power is the reduction of the mass of solar arrays. At present, about 23 percent of a communications satellite mass launched to orbit is dedicated to the power system, approximately the same fraction that is available for payload. An approach under investigation for coupling reduced mass with high efficiency is the use of ultralightweight gallium arsenide solar cells. The Lincoln Laboratory has developed the CLEFT (cleaved lateral epitaxial film transfer) process, which uses a reusable substrate and allows for fabrication of solar cells as thin as 5 μm. The optical absorption of gallium arsenide is such that a few micrometers of thickness are sufficient for light absorption. A gridded-back-contact gallium arsenide cell with an illuminated area of

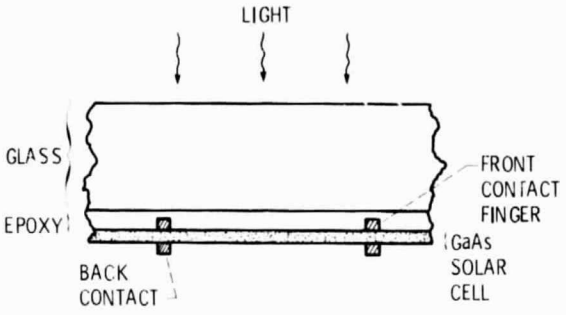

Gridded-back-contact GaAs solar cell

0.51 cm^2 and a thickness of 5.5 μm has achieved 14.3 percent efficiency. The reusable substrate lowers cell costs.

Intercalated-Graphite Fiber Conductors

The electrical conductivity of graphite fibers can be greatly increased by introducing guest molecules between the layers of graphite atoms.

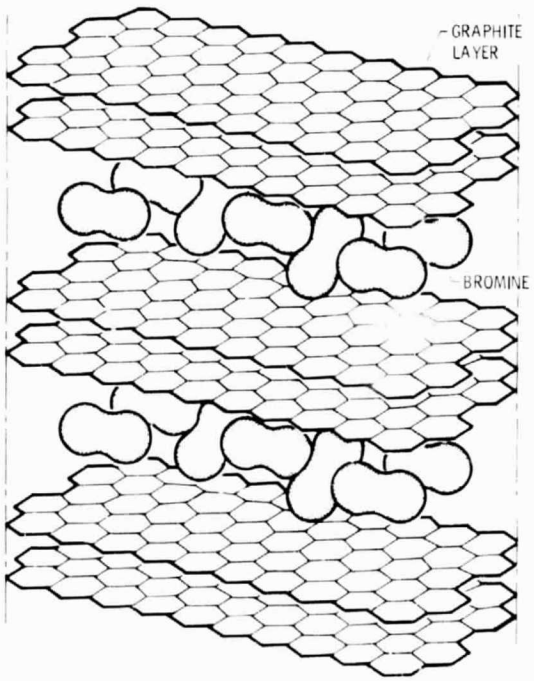

Bromine-intercalated graphite

This process, called intercalation, has been found to produce lightweight, high-strength conductors with electrical conductivities approaching that of copper. However, these intercalation compounds have not proven to be stable, making them unsuitable for aerospace use. At Lewis, graphite fibers intercalated with bromine have shown stability to 200 °C and have conductivities exceeding that of iron. This makes them attractive for use in conductive graphite-epoxy composites for lightweight shielding of aerospace electronics, as dual-purpose materials for electrical conductors and load-bearing structures, and as lightning-strike-resistant aircraft materials. Conventional graphite-epoxy compounds are not adequately conductive to prevent catastrophic failures from lightning strikes.

Free-Piston Stirling for Space Power

The free-piston Stirling engine is being evaluated by Lewis for space power applications in support of the SP-100 program. SP-100 is jointly funded by the Department of Defense, the Department of Energy (DOE), and NASA to develop a 100-kW electrical space power module. In addition, DOE/Oak Ridge National Laboratory is interested in the free-piston Stirling engine for heat-pump applications and has joined with Lewis in funding a limited program at Lewis encompassing generic free-piston technology. The potential advantages of the free-piston Stirling engine for both space and terrestrial heat-pump applications include high efficiency, potential long life and high reliability, no dynamic seals, very low vibration, and simple components.

The overall free-piston Stirling program at Lewis, which includes SP-100 and the DOE generic heat-pump work, has during the past year generated a free-piston Stirling performance and optimization computer code. It has also demonstrated engine vibration amplitude reduction by an order of magnitude. This was accomplished by incorporating a spring-mass dynamic balancing system in a 1-kW operating engine at Lewis. Life testing was begun on a 2.5-kW, 60-Hz engine with a 700 °C heater head temperature by Mechanical Technology Inc. (MTI). This engine successfully completed 1000 hr of endurance testing last year, and testing is continuing toward a goal of 10 000 hr. The cost of testing is shared by the SP-100 program and the Gas Research Institute. MTI has also completed the design of a 25-kW space power demonstrator engine.

As part of the design of the Stirling space power module and its integration into a complete power system, Sunpower Inc. has completed parametric studies to focus on the initial relationship between power-module specific weight and efficiency and engine-heater-to-cooler temperature ratio. This information is important for minimizing complete power system weight and volume for shuttle flights.

Nuclear Space Power Systems

The SP-100 program has identified manned mission scenarios, namely pharmaceutical and materials production, that would require power levels sufficiently high to warrant the use of nuclear power. A detailed study of various alternative methods to supply this power to a manned orbiting facility was also completed. Lewis' analysis of a nuclear dynamic space power system showed that the SP-100 requirements (100-kW power system that weighs less than 3000 kg and fits in one-third of the shuttle bay) could be met by a Stirling or Brayton power conversion system and reactor outlet temperatures of 900 and 1225 K.

As a result of these studies, major contracts were let with Rockwell and General Electric to perform detailed design studies of nuclear Stirling space power systems.

IR-100 30/20-GHz Spacecraft Multiple-Beam Antenna System

Future geosynchronous communications satellites operating in the 20/30 GHz frequency bands will use advanced offset-fed multiple-beam antenna systems to provide multiple radiating fixed-spot and regional coverage scanning beams.

By using many narrow spot beams, such satellite systems will provide for expansion of existing satellite services as well as achieve frequency reuse for conservation of the frequency spectrum. The narrow fixed-spot beams (0.3 beamwidth each) will provide the communications coverage for high-volume traffic between major cities, where each beam will cover an area approximately 200 miles in diameter, and the scanning beams will provide coverage for direct-to-user services to remotely located areas.

Ford Aerospace and TRW Electronic Systems Group, under contract to Lewis, have designed, fabricated, and tested such multiple-beam antennas (Ford, a 20-GHz transmitter; and TRW, a 30-GHz receiver). Each is capable of providing 18 fixed beams to preassigned major cities of the continental United States (CONUS) and 6 scanning beams, where each scanning beam covers approximately one-sixth of CONUS. Both antenna systems use unique concepts in achieving the goals of multiple beams: high gain and good isolation between beams. The Ford offset-fed, dual-reflector antenna system uses doubly curved main and subreflector surfaces to optimize the overall CONUS coverage. The TRW concept uses an additional subreflector to generate dual focal points and thus optimize the overall performance.

Energy Technology

Industry Evaluation of Automotive Stirling Engine

The Stirling engine is being developed as a possible alternative to the spark ignition engine under the Department of Energy's Highway Vehicle System Program. Lewis has project management responsibility for the Automotive Stirling Engine Project. Mechanical Technology Inc., the prime contractor, has designed and built seven experimental mod I engines that have accumulated over 7000 hr of operation. Two of these engines were loaned to General Motors and John Deere and Co. for testing and evaluation during 1984.

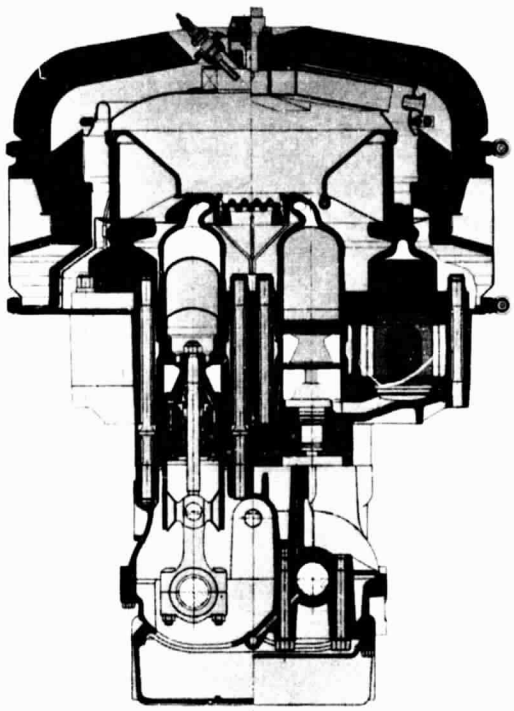

Upgraded mod I automotive Stirling engine

General Motors evaluated their engine in their emissions test facility to determine actual emission levels and fuel economy, in a special wind tunnel to evaluate the cooling system, and on a test track. The engine successfully completed all three phases of testing. It met the current Federal emission levels of 0.41/3.41/1.0 g/m HC/CO/NO_x without the use of a catalytic convertor and attained 22.3 mpg urban and 40.7 mpg highway for a combined value of 28.0 mpg. The cooling system was subjected to a variety of test road loads without showing any distress.

John Deere and Co. will test their engine in the fall of 1984 and will also evaluate its multifuel capability. Operation with a variety of fuels such as gasoline, diesel, and JP-4 is planned.

Stirling Engine Cost Reduction

Under Lewis project management, Mechanical Technology Inc. (MTI) designed a reference

Reference engine system design for automotive Stirling engine

engine system for an automotive Stirling engine that incorporates the best technology expected to be developed over the life of the program. The major features are a four-cylinder, double-acting, V configuration; an annular regenerator/cooler, a ceramic preheater, and a rolling-element drive unit. This design includes a number of features that represent a marked departure from previous designs. The V/annular configuration reduces the number of heater head castings and rotating parts. Manufacturing has been simplified by using a simpler block/cold engine structure.

Pioneer Engineering and Manufacturing Co., under contract to MTI, performed a manufacturing cost analysis of the engine. The basic engine hardware and auxiliaries unique to the Stirling engine system were estimated in detail using 1984 economics for an annual production of 300 000. The installation cost was estimated as $2017, midway between the standard spark ignition engine at $1802 and the diesel engine at $2258.

Ceramic Automotive Stirling Engine

Part of the DOE/NASA Lewis Automotive Stirling Engine Project involves the assessment of advanced technologies. Using ceramics rather than high-temperature metal alloys may have the potential to increase efficiency and decrease cost. Conceptual design studies of ceramic Stirling automotive engines were performed at General Electric and Mechanical Technology Inc. The intent of this work was to define whether a ceramic Stirling engine is feasible, what performance or cost benefits might be derived, and what advances in ceramic technology would be required. Both studies indicated that ceramic Stirling engines are probably feasible, that modest performance gains are possible, and that low-conductivity ceramics (probably oxides) are absolutely vital for key structural components to avoid intolerable conduction losses. The biggest potential gain in using ceramics is not having to use expensive strategic materials such as cobalt, chromium, and nickel. Considerable technology development, particularly in low-conductivity ceramics will be required before the development of a ceramic Stirling engine can be undertaken with confidence.

High-Power-Transistor Analysis Laboratory

A unique high-power-transistor laboratory has been assembled to examine and analyze the characteristics of power transistors for aircraft and space applications. This laboratory will give strong support to the Space Station Program and to other advanced electrical power systems for space power reactors where high-frequency and high-power transistors will be critical elements.

The laboratory is equipped with a power waveform processing system and an operator-interactive graphics computer terminal. The transistors will be driven to maximum ratings but to low stress under low-duty-cycle conditions. Parametric data and characteristic curves will be measured and stored on digital tapes, disks, or internal computer memory for future references and calculations.

Spacecraft Charging Model and Design Guidelines

Electrostatic charging of spacecraft surfaces by space plasmas and subsequent arc discharging have been found to be responsible for the anomalous behavior of a number of geosynchronous spacecraft. In 1976, the U.S. Air Force and NASA established the joint Spacecraft Charging Technology Investigation to solve these problems. Lewis, as lead NASA Center, has

completed development of an analytical design tool and a design guidelines document for spacecraft designers. The design tool is a computer code, called NASCAP (NASA Charging Analyzer Program), that calculates the charging response of complex satellites with multiple surface materials. NASCAP has been validated by ground and flight experiments and has been successfully used to design a number of spacecraft, including Galileo, TDRSS, MARECS, Intelsat VI, and DSP. The code, now available through COSMIC, is in wide use for spacecraft design studies by government and industry in the United States and abroad. It is also being used by the space sciences community as a tool for understanding satellite data.

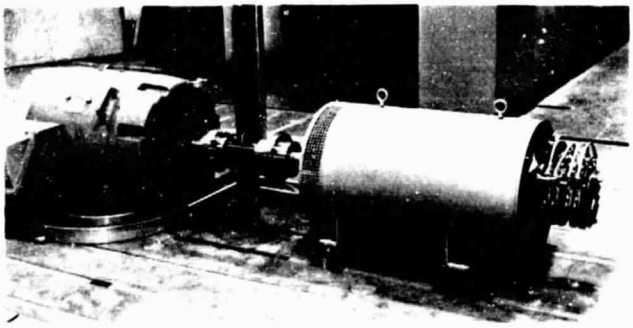

Variable-speed generator testing—from laboratory to wind turbine

The design criteria document, entitled "Design Guidelines for Assessing and Controlling Spacecraft Charging Effects" was compiled by Lewis and Jet Propulsion Laboratory personnel and is now in print as a NASA Technical Paper.

Variable-Speed Generator for Large Wind Turbines

Under the Department of Energy/NASA agreement on large, horizontal-axis wind turbines, Lewis is directing work to improve future wind turbine generator systems. Substantial progress has been made in the development of variable-speed, constant-frequency (VSCF) generators. The turbine rotor speed has been decoupled from the electrical generation process to provide better performance and reliability along with lower cost. Synchronous generators, currently used on large wind turbines, require precise speed control and are rigidly coupled to the utility network. Any speed variations, such as those caused by wind gusts, impose large torque transients on the drive train and rotor, which in turn produce large and potentially transient loads on the machine. The bursts of power from the generator accompanying these transients reduce power quality. Wind turbines using synchronous generators require some form of drive train damping, such as fluid couplings or compliant shafts with blade-tip damping.

Variable-speed generators offer the significant advantage that they can generate constant-frequency power at a constant power level over a wide speed range. Allowing the speed to vary smooths out power surges due to wind gusts and changes in the wind felt by the blades as they rotate past the tower. As a result, the torque and load transients in the drive train and rotor are eliminated. Work on variable-speed generators currently focuses on the cycloconverter-wound rotor alternator concept. A VSCF generator called the Schleif generator was tested both in the laboratory at Lewis and at the Plum Brook Station. During laboratory tests using a dc drive motor to simulate the wind turbine, the Schleif system was optimized with respect to variable speed range, control response, and power quality. Later at Plum Brook the Schleif was tested in the Mod-0 wind turbine. Preliminary tests confirm the expected advantages of variable-speed generation.

Title	Lewis contact	Phone number, (216) 433-4000, extension—	Headquarters program office
Radiation Exposure in LEO/GEO Transfers	Sol H. Gorland	5113	OAST
High-Pressure Turbopump Impeller Seal	Robert C. Bill	389	OAST
Large Vaporizers for Mercury Ion Thrusters	Ralph J. Zavesky	5350	OAST
Flow Analysis of Turbine Exhaust Duct	Louis A. Povinelli	5212	OAST
Measuring Stress in Thin Films	Maris A. Mantenieks	6851	OAST
Simplified Power Processor for Ion Thrusters	Maris A. Mantenieks	6851	OAST
Spacecraft Charge Control	Fred F. Terdan	233	OAST
Thermal Barrier Coatings for Rocket Thrust Chambers	Richard J. Quentmeyer	5171	OAST
IAPS 9000-hr Ground Test Completed	Charles A. Low, Jr.	6631	OAST
Advanced Photovoltaic Experiment	Richard W. Vernon	5186	OAST
High-Voltage, High-Power Remote Power Controllers	John C. Sturman	6655	OAST
Advanced-Design Nickel-Hydrogen Cells	Lawrence H. Thaller	5260	OAST
Synthetic Battery Cycling of Sodium-Sulfur Cells	Lawrence H. Thaller	5260	OAST
Advanced Electrocatalysts for Phosphoric Acid Fuel Cell Powerplants	Marvin Warshay	5251	OAST
Simulation of Phosphoric Acid Fuel Cell Powerplants	Marvin Warshay	5251	OAST
Verification of Electric Utility Fuel-Cell-Stack Technology	Marvin Warshay	5251	OAST
Advanced Alkaline Fuel Cell Technology	Lawrence H. Thaller	5260	OAST
Ultralightweight Gallium Arsenide Solar Cells	David J. Brinker	7308	OAST
Intercalated-Graphite Fiber Conductors	Bruce A. Banks	5222	OAST
Free-Piston Stirling for Space Power	Jack G. Slaby	6824	OAST
Nuclear Space Power Systems	Ronald J. Sovie	793	OAST
30/20-GHz Spacecraft Multiple-Beam Antenna System	Royce W. Myhre	713	OSSA
Industry Evaluation of Automotive Stirling Engine	James G. Dudenhoefer	258	OAST
Stirling Engine Cost Reduction	William K. Tabata	363	OAST
Ceramic Automotive Stirling Engine	William A. Tomazic	258	OAST
High-Power-Transistor Analysis Laboratory	Long V. Truong	5221	OAST
Spacecraft Charging Model and Design Guidelines	Carolyn K. Purvis	5224	OAST
Variable-Speed Generator for Large Wind Turbines	Darrell H. Baldwin	6160	OAST

Materials and Structures

Passive Eddy Current Damper Technology for Cryogenic Machinery

Eddy current damper technologies provide a means of dissipating unwanted shaft vibrations in cryogenic turbomachinery, where the low temperatures preclude the use of more conventional damping mechanisms. A rotating test apparatus was designed and fabricated to evaluate the performance of an eddy current damper operating fully immersed in liquid nitrogen at -197 °C. The damper consists of four equally spaced C-shaped permanent magnets. Four pie-shaped copper segments are attached to a flexible cylinder known as a squirrel-cage spring. The copper segments are located so that each is centered between the north and south pole faces of the magnets. The cylindrical spring is fixed to the machine frame at one end and houses the outer race of a ball bearing at the opposite end. The shaft can be unbalanced with a known weight at a prescribed distance from the center. The rotating unbalance force causes the copper segments to vibrate in a precessional orbit. When magnetic lines of force are cut by the vibrating conductor, an induced flux field is generated that opposes the motion. This damping force acts much like the damping force produced by viscous liquid. The magnitude of the damping is greatly enhanced when both the magnets and conductors are immersed in a cryogenic liquid, in this case liquid nitrogen.

In typical test results the amplitude of vibration at the fundamental resonant frequency was reduced to almost one-half that for the undamped case.

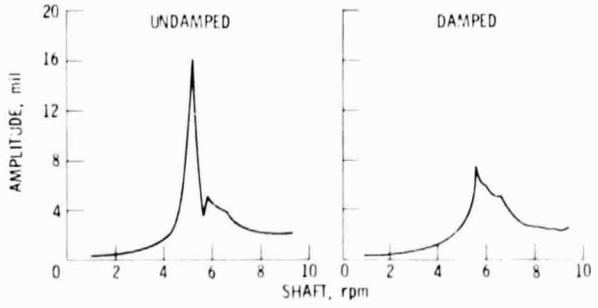

Measured response of undamped and damped rotors

Swept-Fan-Blade Flutter

The first studies of the effect of sweep on fan blade flutter were made by applying the analytical methods developed for aeroelastic analysis of advanced turboprops. Two methods were used: an approximate structural model in which the blade is represented by a swept, nonuniform beam, and a finite-element technique to conduct modal flutter analysis. For both methods the unsteady aerodynamic loads were calculated by using two-dimensional cascade theories modified to account for sweep. An advanced fan stage with 0, 15, and 30 degrees of sweep was analyzed. It was found that sweep has a beneficial effect on predominantly torsional flutter and a detrimental effect on predominantly bending flutter. This detrimental effect was significantly destabilizing for 30 degrees of sweep. Experimental results are in good qualitative agreement.

IR-100 Photo-Optical Blade Vibration Data Acquisition System

A system developed at Lewis for measuring the vibrations of the blading on operating turbomachinery has won an IR-100 award for 1984 from Research & Development Magazine. The system monitors the passage of turbine engine blade tips as they pass a fixed array of light-emitting diodes and photoreceptors. The precise time that each blade passes any sensor is recorded with a resolution as high as 30 ns. The information obtained from an array of such sensors is used to simultaneously reconstruct the time-deflection history (or vibration response) of each blade tip on the turbine rotor. With measurements made in each of three horizontal planes the system can discern blade tip bending, torsion, and camber line deformation. With a 2048-point sample base as a selected option, a 64-blade stage operating at 18 000 rpm generates 393 216 data points in 70 ms and fully measures the vibration characteristics of a bladed disk assembly.

The measurement system provides a very high sample rate and can discern the total vibration

pattern on an assembly of blades imbedded within operational turbomachinery. The unique way that measurements are made provides high accuracy as a bladed disk operates at higher speeds. The system samples blade positions at rates as high as 2 MHz asynchronously and automatically corrects for "missed" blades and nominal misalignments. An array of special-purpose microcomputers allows for a variety of alternative sampling modes: for measuring only specific blades or for enhancing the frequency resolution. None of these capabilities exist within other systems; there is no comparable measurement system in existence.

Effects of Different Rub Models on Gas Turbine Rotor Dynamics

In an aircraft gas turbine there are many instances in which the rotating parts can rub the case. A large frictional force can be generated that can drive this rotor into a whirling motion at very high speed. This can be very dangerous. An improved method for predicting the stability limits of gas turbine engines has been developed at Lewis. The response of turbine engine rotors to two blade tip-seal interference rub models was studied by computer simulation. The first model, an abradable seal rub model, is based on an energy-loss-per-unit-volume theory. It is applicable to a ceramic turbine blade tip seal. The second, a smearing model, is based on viscous hydrodynamic theory. It is applicable to a metallic turbine blade tip seal.

The results from these two models were compared with those from a previously studied model based on dry friction theory. The abradable model was very sensitive to small changes in the energy per unit volume. Once a threshold was exceeded, the rotor went into backward whirl. The amplitude seemed to grow without limit. This was similar to the dry friction model when the coefficient of friction exceeded a particular threshold. The smearing model was not as sensitive to small changes in the viscosity, but a threshold viscosity was found. When it was exceeded, the rotor went into backward whirl, but the amplitude seemed to grow to a finite limit. This new analytical tool provides information that will allow the design of rotor surface rub systems to minimize the possibility of catastrophic rub-induced rotor system failures.

High-Temperature Erosion Rig

The thermal efficiency of gas turbine engines depends on maintaining airfoil profile integrity and tight clearances between blade tips and gas path seals. Efficiency gains can also be realized in the turbine by using ceramic-coated hardware, thus allowing higher combustion temperatures while minimizing cooling requirements that penalize compressor efficiency. Damage to these components in the form of solid-particle erosion can drastically affect overall engine performance.

The high-temperature erosion rig provides a repeatable simulated jet engine turbine environment in terms of temperature and gas velocity and the erosive grit that is introduced into the gas stream. When a simulated gas path seal specimen of plasma-sprayed yttria-stabilized zirconia is used, temperatures to 2900 °F can be achieved, with particle velocities as high as 1000 ft/s. The data generated by successive tests on specimens provide the steady-state erosive

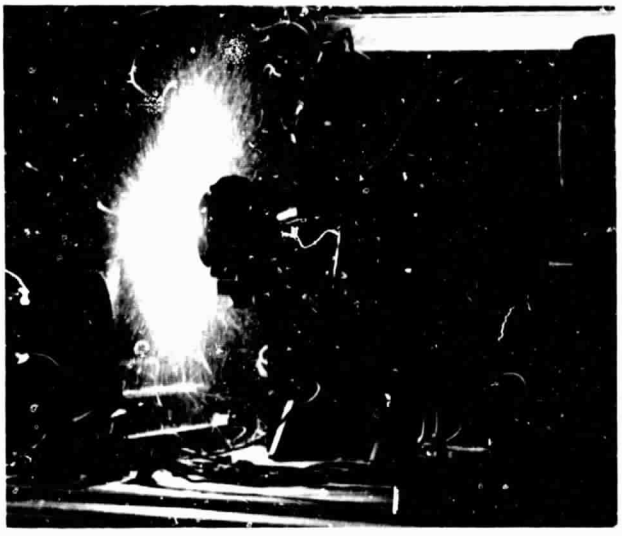

High-temperature erosion rig in operation

performance as a function of impingement angle, temperature, particle velocity, and other test rig and specimen configuration parameters. Parametric studies with the test variables can be used to optimize the erosive performance of critical engine components as a function of the environmental conditions expected.

Method for Fabricating All-Zirconia Gas Path Seals

A new method for fabricating all-zirconia turbine tip gas path seals has several advantages over the current system of a metal shroud with a plasma-sprayed zirconia hot face. These include greater insulation capacity, better control of shape and size distribution of the pore phase (resulting in more consistent mechanical properties), and lower thermal strains.

The method consists of tape casting thin zirconia sheet (0.010 in. thick), laminating these castings, and consolidating them under uniaxial pressures to 10 000 psi and sintering at 3000 °F. The composition of each layer can be controlled independently, and a burnout phase is allowed in order to leave an optimum-geometry pore phase for rotating-blade-tip-stationary-gas-path-seal rubs. Zirconia with a refractory stabilizer (e.g., yttria) can be incorporated for the hot face, and zirconia with a stabilizer that allows transformation toughening (e.g., calcium) can be incorporated for the supports. The fact that the seal is entirely based on zirconia allows isothermal high-temperature heat treatments to develop the toughened microstructure.

Successful experiments demonstrate that the tape casting, lamination, and sintering of zirconia are viable fabrication methods for all-zirconia seals.

Nondestructive Characterization of Structural Ceramics

Gas turbine engines can be made more efficient by making them from ceramics such as silicon carbide and silicon nitride. These materials can operate at higher temperatures than currently used metals. However, ceramics are more vulnerable to fracture. They also exhibit wide variations in mechanical strength, generally because microflaws and nonuniformities are introduced during the processing of ceramic components. Nondestructive evaluation techniques are needed to ensure that ceramic parts used in turbine engines are free of serious flaws. Moreover, these techniques are needed to characterize ceramic parts at different processing stages from the "green" state to the fully densified, finished state. Microflaw populations in ceramics impose severe demands on nondestructive evaluation technology.

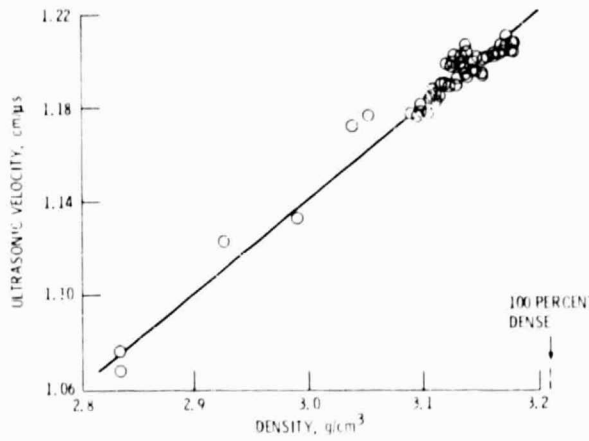

Linear relation between ultrasonic velocity and bulk density of ceramics

A program being pursued at Lewis is dedicated to the development of advanced nondestructive evaluation techniques for structural ceramics. High-resolution film and microfocus *x* radiography and high-frequency ultrasonic techniques are being investigated. These include velocity and attenuation measurements to detect density and strength variations. Radiography and ultrasonic microscopy are being applied to image microflaws and microstructural variations. One of the most important results of this program has been its feedback contribution to ceramics processing research. Close teamwork pinpointed processing conditions that produce unacceptable ceramics. It was discovered that sintered

ceramics often contained a low-density core surrounded by a high-density case. This case/core problem was attributed to thermal diffusion gradients during sintering. The problem was remedied by closely coordinating ceramic processing and nondestructive evaluation.

Structural Dynamics Code for Entire Turbine Engines

The Turbine Engine Transient Response Analysis (TETRA) code recently developed by Lewis for analyzing transient vibrations of entire turbine engines as coupled structural dynamic systems has been significantly enhanced by the addition of a squeeze-film damper module and an output plotting package. This code uses previously calculated modal constants of major engine components as input. It then solves the equations of motion of each component by a time integration method, taking into account at each step the forces exerted at physical connection points between components, such as bearings and blade-tip rub points. Deflections, stresses, connecting point forces, and induced blade vibration can be found.

TETRA was developed to analyze the transient response to events such as blade loss but can also be used to explore the effects of manufacturing imbalance. With the newly added squeeze-film damper module it is now possible to study the control of rotor dynamics vibration and the integrity of the engine after massive blade loss.

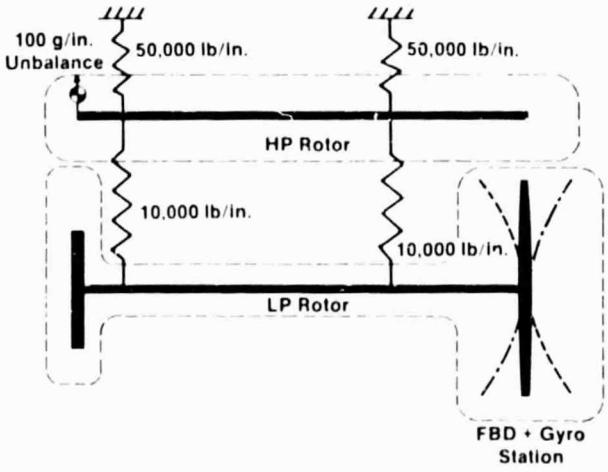

TETRA two-rotor demonstration model

New Method of Power Transmission Shaft Design

A long-standing objective in the design of power-transmitting shafts is to reduce their size and weight without sacrificing operational reliability. A shaft design method has been developed that allows the designer to quickly assess the effect of key operating variables and material selection on shaft fatigue life and size. This method, based on a stress-life approach, accounts for both constant- and variable-amplitude loading histories and can be used to size shafts for limited life applications. It is applicable to any combination of cyclic bending and torsional loading. Residual stress, press-fitted collars, and corrosion fatigue are among the factors considered. The method lends itself to computer-aided design of both aerospace and industrial shafting.

Analytical Method to Predict Aircraft Gearbox Efficiency

A power loss prediction method has been developed to analyze the performance of external and internal involute spur gears with teeth of either standard or nonstandard proportions. This analysis accounts for the effects of modified addendums, tooth thickness, and nonstandard center distances in addition to normal geometric parameters such as gear diameter, pitch, and pressure angle. The flexibility of this method allows, for the first time, the analysis of recess-action and high-contact-ratio gears. These gears have received much attention for use in aircraft applications because of their smoother operating characteristics and, in the case of high-contact-ratio gearing, higher load-carrying capacity.

This method was used to predict the efficiency of a T-56 turboprop gearbox, used on some 13 000

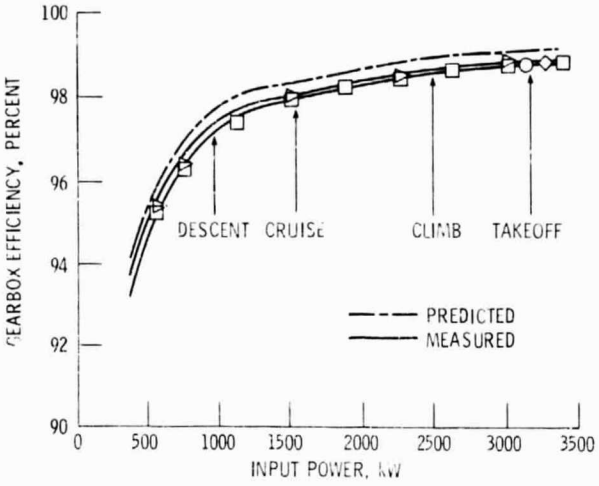

Comparison of predicted and measured T-56 gearbox efficiency over complete flight spectrum

military and commercial aircraft, including the Lockheed C-130 and Electra transports. Predicted efficiency showed relatively good agreement with measured data across the complete flight spectrum. A breakdown of component losses indicated that the oil pumps account for a major portion of the total system loss.

Nonlinear Analysis for High-Temperature, Multilayered Fiber Composite Structures

The idea of using advanced high-temperature composite materials in turbine engine hot sections is becoming more attractive. These materials allow higher operating temperatures and thus improve engine performance and efficiency while enhancing, or at least maintaining, component durability. For example, the tungsten-fiber-reinforced superalloys (TFRS) have been identified as potential first-generation composite turbine blade and vane materials by virtue of the excellent complementary properties they provide. To adequately investigate the feasibility of using materials such as TFRS for turbine hot-section components, better analytical tools are needed. Complex physics associated with these applications must be accounted for.

In response to this need research was begun to develop a computational tool able to quantitatively assess the mechanical performance and structural integrity of advanced high-temperature composites in turbine engine applications. It resulted in the development of an integrated analysis capability (nonlinear COBSTRAN) that incorporates a nonlinear thermoviscoplastic material model, composite micromechanics theory, laminate theory, and global finite-element structural analysis. Its present capability is tailored for the nonlinear analysis of TFRS turbine blade and vane structures.

Interply Layer Effects on "Free Edge" Stress Field

The presence of free edges (edges that are not loaded or otherwise restrained) in composite laminates often gives rise to a complex three-dimensional stress field with steep gradients. This field has been studied experimentally and analytically to a considerable depth during the last 15 yr. It is thought that delaminations and matrix microcracking occur near free edges because of the steep interlaminar stress gradients as the free edge is approached. However, much controversy still exists regarding the nature and magnitude of the interlaminar free-edge stresses. For analysis purposes the free-edge region of a composite laminate is usually modeled as homogeneous anisotropic layers sharing common boundaries. In reality, however, there exists a thin (about a few percent of the ply thickness), soft matrix layer between the plies. The effect of such a layer on the free-edge stress field must be considered to completely describe the stress field as the free edge is approached and also to understand the significance of the apparent singular behavior of some of the interlaminar stress near the free edge.

Recently the general-purpose, finite-element program MSC/NASTRAN was used at Lewis to study the interply layer effects on the free-edge stress field of symmetric angleplied laminates subjected to uniform tensile stress. The free-edge

region was modeled as a separate substructure (superelement) for easy mesh refinement and the flexibility to move the superelement along the edge. The results indicated that the interply layer significantly reduces the stress intensity at the free edge. Another important observation of the study is that the failures observed near free edges of these types of laminates could have been caused by the interlaminar shear stresses.

Dynamic Stress Analysis of Smooth and Notched Fiber Composites

Testing of smooth and notched flexural specimens continues to be popular for characterizing and qualifying fiber composites. Such testing is simple and adaptable to adverse environments, uses simple equations for data reduction, and is based on written American Society for Testing Materials standard testing procedures. Flexural specimen testing also forces the material to respond like a structure by simultaneously subjecting it to tensile, compressive, and shear stresses.

Fracture is a dynamic event and, as such, is a very complex process. For a complete understanding of the phenomena involved in fracture the local dynamic stress field must be described in detail. This requires the use of a complex transient analysis involving direct time integration. Lewis has recently performed a detailed analysis of the dynamic stress field in smooth and notched Charpy specimens.

Simplified Composite Micromechanics Equations

The several strengths (stresses at fracture) of unidirectional composites are fundamental to the analysis and design of fiber composite structures. Some of these strengths are determined by physical experiments. Others are not easily amenable to direct measurement by testing. In addition, testing is usually time consuming and costly and requires an existing composite.

Furthermore parametric studies of the effects of fiber volume ratio on properties such as impact resistance and fracture toughness can be made only by an extensive series of tests. Another approach is to use composite micromechanics to derive equations for predicting composite strengths based on constituent (fiber and matrix) properties. Over the last 20 yr, composite micromechanics has been used to derive equations for predicting selected composite strengths. However, these equations are not readily available since equations for different strengths are scattered throughout the literature and equations for predicting many strength-related properties are not available in the literature.

Recently a unified set of composite micromechanics equations was developed at Lewis. This set includes simple equations for predicting ply (unidirectional composite) strength by using constituent properties. Equations developed include strengths (in plane and through the thickness), flexural strength, "fracture toughness," and impact resistance. Also, equations were developed to predict the effects of moisture and temperature, or hygrothermal effects. The equations of this unified set are summarized in subsets corresponding to each of the strength, "fracture toughness," impact resistance, and hygrothermal effects. The equations of each subset are summarized in chart form. This allows the equations for each subset to be on one page for convenience of use and identification of various interrelationships. Typical

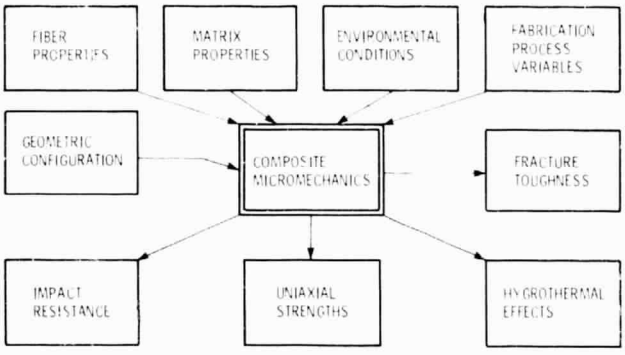

Concepts, models, and equations used to predict composite strengths

constitutent material properties are included so they can be used in the equations for numerical calculations.

Linear Approximations to Three-Dimensional Inelastic Analysis

Hot-section durability problems appear in a variety of forms, ranging from oxidation/corrosion, erosion, and distortion (creep deformations) to fatigue cracking. Even modest changes in shape, from erosion or distortion of airfoils, for example, can lead to measurable performance deterioration that must be accurately predicted during propulsion system design to ensure long-term efficiency. Larger distortions introduce serious problems such as hot spots and profile shifts resulting from diversion of cooling air, high vibratory stresses associated with loose turbine blade shrouds, and difficult disassembly/reassembly of mating parts at overhaul. These problems must be considered and efforts made to eliminate their effect during engine design and development. The initiation and propagation of fatigue cracks represent a direct threat to component structural integrity and must be thoroughly understood and accurately predicted to ensure safe and efficient engine operation.

Pratt & Whitney Aircraft, in partnership with United Technologies Research Center, MARC Analysis Corporation, and the State University of New York at Buffalo, under contract from Lewis, is conducting a three-dimensional inelastic analysis methods development program. During the first year of this program a series of new computer codes embodying a progression of mathematical models was developed for the streamlined analysis of combustor liners and turbine blades and vanes. These models address the effects of high temperature and thermal/mechanical loadings on the local and global structural behavior of these components. Eventually these codes, MOMM (Mechanics of Materials Model), MHOST (MARC-HOST), and BEST (Boundary Element Stress Technology), will be available from COSMIC.

Interply-Layer Progressive Degradation Effects

Fiber-reinforced composites are optimally utilized when they are required to resist or transfer only in-plane loads. Fibers are oriented in different layers (plies) to resist these in-plane loads either in tension or compression. The different plies are held together by the interply (interlaminar) layers (matrix), which provide the composite with the structural integrity required to resist the in-plane loads. Degradation of the interply layer will therefore affect composite structural integrity and, as a result, is receiving considerable research attention. Interply degradation generally occurs as delaminations or progressive weakening of the interply layer. In either case, the composite angleplied laminate will most likely behave like a stack of individual layers (beams) instead of a composite. Such behavior dramatically degrades out-of-plane structural response such as flexural deflections (bending), buckling, vibration, and impact.

Lewis has recently been computationally determining and assessing the effects of interply layer progressive weaking (degradation) on various structural responses of a composite beam. The structural responses of interest include bending, buckling, free vibrations, periodic excitation, and impact. Finite-element

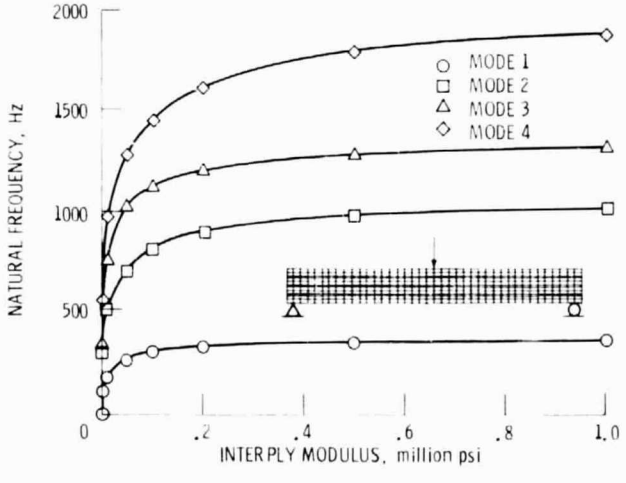

Interply degradation effects on vibration frequencies

analysis was used. The results obtained show that interply layer degradation generally has a negligible effect on composite structural integrity unless the interply layer modulus degrades to about 10 000 psi or less.

ICAN: Integrated Composite Analyzer

The most cost-effective way to analyze and design fiber composite structures is through the use of computer codes. Composite analysis computer codes have concentrated on "classical" laminate theory. Extensive research has been conducted at Lewis to develop composite mechanics theories and analysis methods that account for environmental effects and are applicable to intraply and interply hybrid composites and combinations thereof. Most of these theories are represented by simplified equations that have been corroborated by experimental results and finite-element analyses. The composite mechanics theories with their respective simplified equations constitute a structured theory that is "upward integrated" from material behavior space to structural analysis; and "top-down traced" from structural response to material behavior space. This structured theory has been incorporated into a computer code called ICAN (Integrated Composite Analyzer). The ICAN computer code is efficient in predicting the structural response of multilayered fiber composites. The code also performs detailed laminate stress analyses under complex loading conditions including hygrothermal environments.

Select Composites for Space Applications: A Mechanistic Assessment

Because the use of fiber composites in space applications is increasing, reliable methods are needed for predicting their properties in the space environment. Particular attention must be paid to the thermocyclic behavior of fiber composites when subjected to temperatures ranging from cryogenic, or deep space, to the relatively high temperatures due to solar heating.

The Lewis-developed computer code ICAN (Integrated Composite Analyzer) has been used to predict the thermal and mechanical properties of select fiber composites in cryogenic environments. The material systems, laminate configurations, cryogenic temperatures, and predicted properties selected for this analysis are relevant to current space applications. The thermal properties predicted were heat capacity, heat conductivity, and coefficient of thermal expansion. The mechanical properties predicted included moduli, both elastic and shear, and Poisson's ratio. These predicted properties and the residual stresses were calculated and presented graphically as a function of laminate configuration, fiber volume ratio, and temperature.

Finite-Element Substructuring for Composite Micromechanics

The need for techniques to predict composite micromechanics properties more accurately for the design and analysis of composite systems is becoming imperative. Composite equations are a simple and quick way to predict these properties—however, with somewhat questionable results. Another technique is the finite-element method. Conventional finite-element analyses have been performed for a few specific properties. However, advanced finite-element techniques such as hierarchical substructuring have not been used although these are the only viable methods to describe the detailed microstress/strain fields in multifiber composites.

Finite-element hierarchical substructuring was used at Lewis to predict unidirectional fiber composite hygral (moisture), thermal, and mechanical properties for boron/HN-epoxy, S-glass/IMHS-epoxy, and AS/IMHS-epoxy. COSMIC NASTRAN and MSC/NASTRAN as well

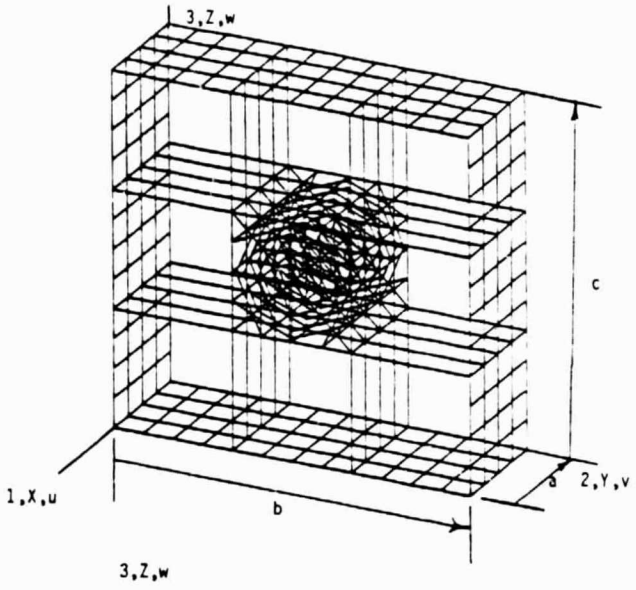

Oblique view of nine-cell superelement model

as three-dimensional isoparametric brick elements and two distinct models were used to perform the finite-element analysis. The first model consists of a single cell (one fiber surrounded by a matrix) to form a square. The second model uses the single cell and substructuring to form a nine-cell square array. An independent computer program consisting of the simplified micromechanics equation was developed to predict the hygral, thermal, and mechanical properties for this comparison. All three methods of prediction were in agreement, so the simplified micromechanics approach appears promising.

Progressive Fracture of Fiber Composites

Predicting composite durability and structural reliability depends on being able to characterize defects and subsequent defect growth to fracture. Developing this capability involves developing techniques and methods for determining combined stress states in composite laminates and the subsequent application of appropriate failure criteria.

Over the past several years, unique capabilities have been developed at Lewis including the Composite Durability Structural Analysis (CODSTRAN) computer code and the real-time ultrasonic C-scan (RUSCAN) experimental facility. CODSTRAN is an upward-integrated mechanistic method for predicting durability and defect growth in composites. The program incorporates composite mechanics, laminate theory, structural analysis (finite element), and fracture criteria modules. RUSCAN is a nondestructive testing apparatus that can scan a specimen or structure under an applied load for defects and damage. These two capabilities, along with analysis by scanning electron microscopy, were used to characterize progressive fracture of composites.

CODSTRAN and RUSCAN have proved to be effective. Evidence of this is the good agreement between observed (via RUSCAN) and predicted (by CODSTRAN) fracture patterns and crack-

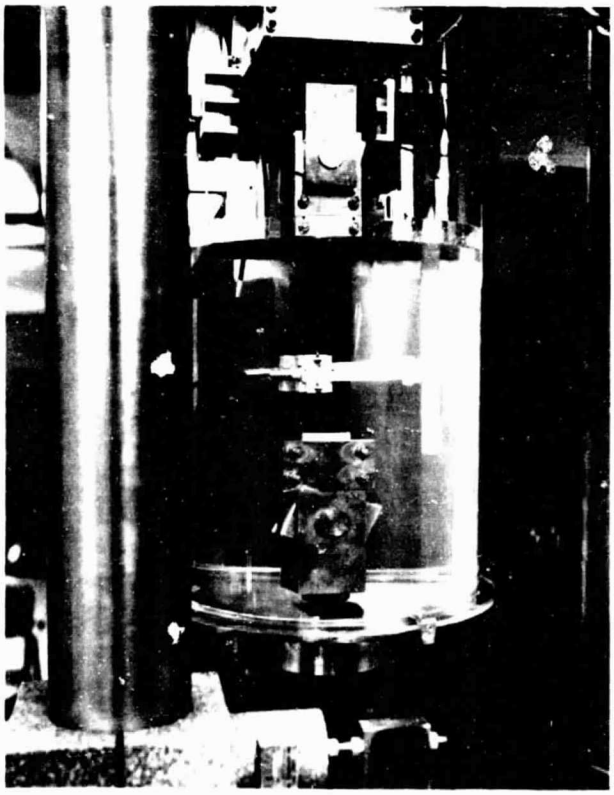

Notched specimen sample in RUSCAN load frame

opening displacements. Similarly CODSTRAN-predicted fracture modes match fracture surfaces seen under the scanning electron microscope. Significantly, results indicate that the laminate mechanical response, progressive fracture, and fracture load in graphite fiber/epoxy composites are independent of the defect type studied (slot or hole).

Lower-Curing-Temperature PMR Polyimides

The novel class of polyimides known as PMR (*in situ* polymerization of monomer reactants) polyimides was developed by investigators at Lewis in response to the need for high-temperature-resistant polymers with improved processability. The PMR matrix designated as "PMR-15" has achieved wide acceptance because of its excellent balance of processability and thermo-oxidative stability. The final cure of PMR-15, however, must be conducted at 600 °F, which exceeds the temperature capabilities of many industrial curing facilities. Recent studies conducted at Lewis have identified a PMR composition, designated as "PMR NV-600," that can be processed at 500 °F.

Unidirectional Celion 6000 graphite fiber/PMR NV-600 composites exhibited room-temperature and short-term 600 °F mechanical properties essentially equivalent to those of PMR-15 composites. Although the 600 °F flexural strength retention of the PMR NV-600 composites was slightly lower than that of PMR-15 composites, their weight loss characteristics after exposure in air at 600 °F were virtually identical.

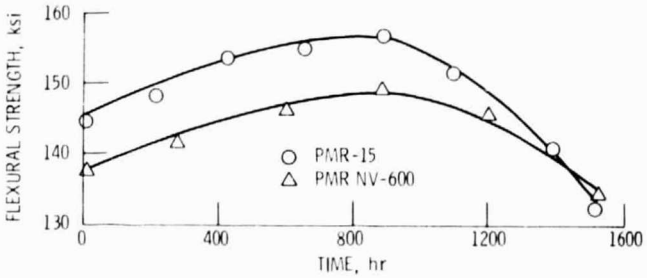

Flexural strength of PMR NV-600

Better Understanding of Friction and Wear Properties of Ferrites

Fundamental studies have been made of the role of environment, composition, and crystallography in the friction and wear of ferrites in contact with metals, magnetic tapes, and themselves. It was found that the removal of adsorbed films from the

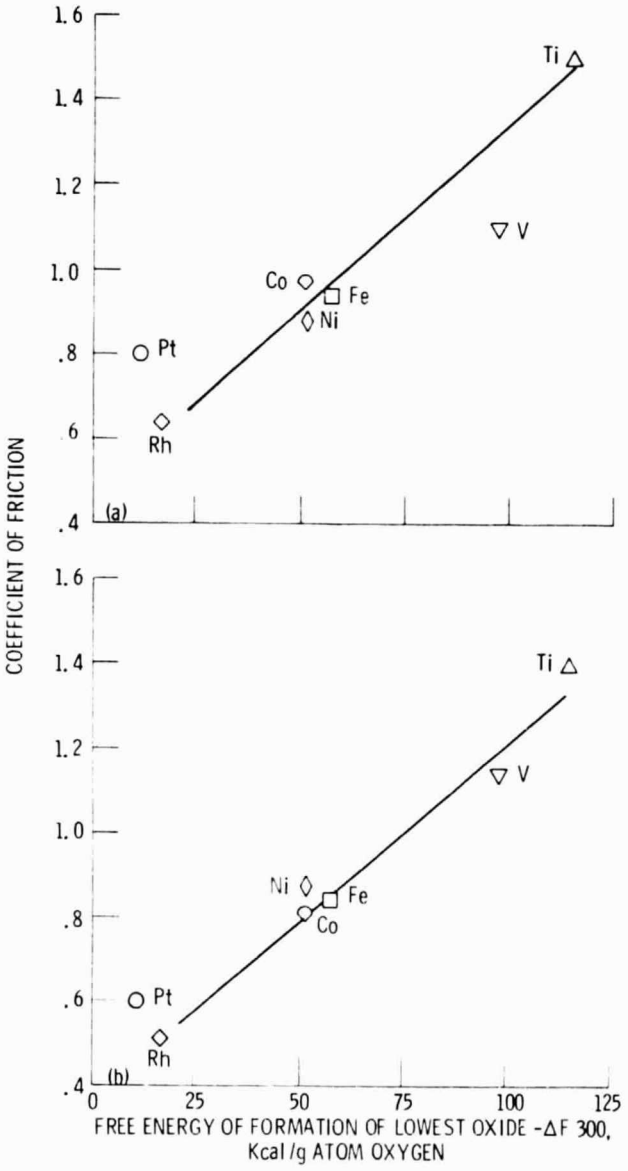

Coefficients of friction for various metals in contact with (a) Ni-Zn and (b) Mn-Zn ferrites

surfaces of the ferrites resulted in very strong interfacial adhesion and high friction in ferrite-to-metal and ferrite-to-magnetic-tape contacts. The ferrite-metal bond at the interface was primarily a chemical bond between the metal atoms and the oxygen ions in the ferrite surface. The strength of these bonds was related to the oxygen-to-metal bond strength in the metal oxide. The more active the metal, the higher was the coefficient of friction. Under both adhesive and abrasive conditions the friction and wear properties of the ferrites were related to their crystallographic orientation. With ferrite-to-ferrite contact the mating of highest atomic density (most closely packed) directions on matched crystallographic planes (i.e., ⟨110⟩ directions on {110} planes) resulted in the lowest coefficient of friction. Under abrasive conditions the anisotropic friction of ferrites did not correlate with the hardness, while anisotropic wear was inversely proportional to the hardness of the wear surface on abraded ferrites.

Surface Roughness Effects in Elastohydrodynamic Contacts

The effects of surface roughness on the film shape in elastohydrodynamically lubricated contacts were studied theoretically. The analysis was based on a Reynolds equation modified through flow factors determined by the statistical properties of the surface topography. Within the approximation of the second-order perturbation approach to stochastic flow, only two parameters govern the pressure developed by the film. In nondimensional form these are the ratio of nominal film thickness to rms roughness amplitude and the ratio of the correlation lengths parallel and perpendicular to the lay direction of the surface texture.

The formalism was applied to the lubrication of cylindrical rollers—one dimensional or line contact—and carefully converged results for physical quantities such as film shape, pressure distribution, and traction coefficients were obtained. It was found that surface asperities elongated in the flow direction by a factor of 2 or more decreased the minimum film thickness at constant load. For smaller elongations, including isotropic asperities, film thickness increased. Although this agrees qualitatively with the work of others, the size of the effect was an order of magnitude smaller than expected. For roughness amplitudes physically reasonable in the present lubrication model, film thickness was changed by only 1 or 2 percent. The traction coefficient was altered by approximately the same amount but in this instance, longitudinal roughness increased traction and transverse or isotropic roughness decreased it. To present accuracy, computations of the height of the elastohydrodynamic pressure spike were consistent with a spike independent of the roughness parameters. However, there was some evidence of a trend to lower spikes for longitudinal cases and higher spikes for isotropic or transverse roughness.

Oxidation/Corrosion Study of Stirling Engine Alloys

The oxidation and corrosion resistance of candidate Stirling engine heater-head-tube alloys was investigated under conditions simulating automotive applications of the Stirling engine. Duplicate sheet specimens of 16 alloys were evaluated for 3500 hr under cyclic conditions at 820 °C in a Stirling engine simulator materials test rig. The specimens were heated for 5-hr cycles and specific weight change was measured and fitted to an attack parameter equation. X-ray diffraction, metallographic, and electron microprobe analyses were also made.

Three of the alloys, CG-27, Sanicro 32, and 12RN72, were judged to be leading candidate heater-head-tube alloys. On the basis of other considerations such as low strength high cost, and high strategic metal content the next best seven alloys with excellent or good environmental resistance were given much lower priority. Alloy CG-27 was given the highest priority because of its superiority at the high operating temperatures, 820 to 870 °C, of current designs for the

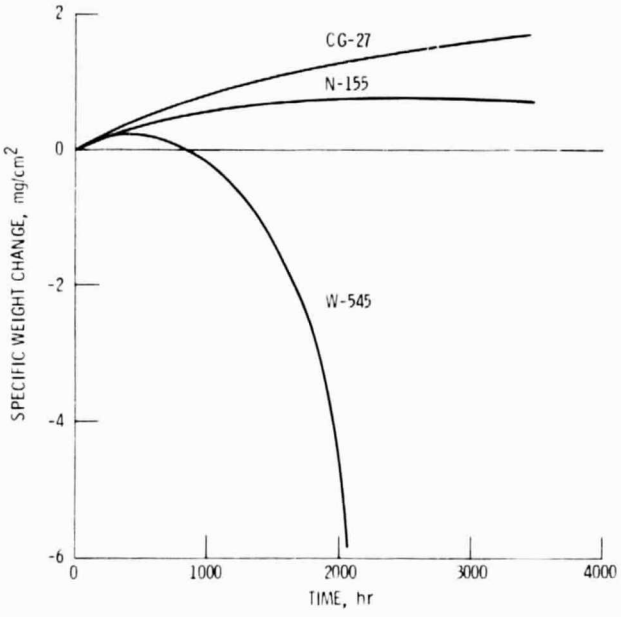

Cyclic oxidation behavior of candidate Stirling engine heater-head-tube alloys

automotive Stirling engine. Electron microprobe analysis of the oxide scales formed on CG-27 indicated an outer surface oxide rich in iron, nickel, and aluminum; an intermediate oxide scale rich in chromium and titanium; and an aluminum-rich subscale adjacent to the metal. Beneath the oxide layers was a zone of alloy substrate that exhibited internal oxidation, primarily of aluminum along with some titanium. Of the alloys investigated, CG-27 contained the smallest amount of the strategic metal chromium (13 percent) and none of the strategic metal cobalt. By comparison, alloy N-155, used in current prototype engines, contains 20 percent chromium and 20 percent cobalt. Alloy CG-27 has been recommended and accepted as the heater-head-tube material for upgraded mod-I automotive Stirling engines.

Super Single-Crystal Superalloys

Recent studies have shown that rapid directional coarsening (linking) of γ', commonly called γ' rafting, greatly enhances high-temperature creep resistance (a factor of 4 increase in creep life) over materials that do not exhibit rapid γ' rafting. The present research has demonstrated that directional coarsening, and the subsequent creep properties that result, can be altered significantly by changes in the initial microstructure prior to creep testing.

A range of γ' particle sizes were produced in different single-crystal specimens by changing the quench rate from the homogenization temperature or by giving the material an additional aging treatment. The oil-quenched crystals, which had the finest γ' size, exhibited the most rapid rafting rate during creep. The closely spaced γ' particles in this condition may have hastened the development of the rafts because the distance for diffusion was reduced. In addition, the rafting kinetics were improved by the lack of interfacial dislocations, which reduce the driving force for the directional coarsening process.

Since the γ' particles in this alloy merge laterally into plates without thickening, the raft thickness equalled the initial γ' size. The single crystals with the finest γ' size had the longest creep lives because the resultant rafted structure had the most γ-γ' interfaces per unit volume of material and this provided additional barriers to mobile dislocations.

Life Prediction Model for Advanced Thermal Barrier Coatings

An oxidation-cooling stress life prediction model developed at Lewis has been verified in cyclic furnace tests of thermal barrier coatings applied over low-pressure-plasma-sprayed bond coats. In a cooperative program with the General Electric Company, a 0.04-cm-thick layer of ZrO_2-$8Y_2O_3$ ceramic was plasma sprayed at atmospheric pressure over a 0.01-cm-thick NiCrAlY bond coat. Specimens were cycled between room temperature and 1100 °C with heating cycles of 1, 6, and 20 hr. The lives, or numbers of cycles to failure, and the oxidative weight gains as a function of time were recorded and compared

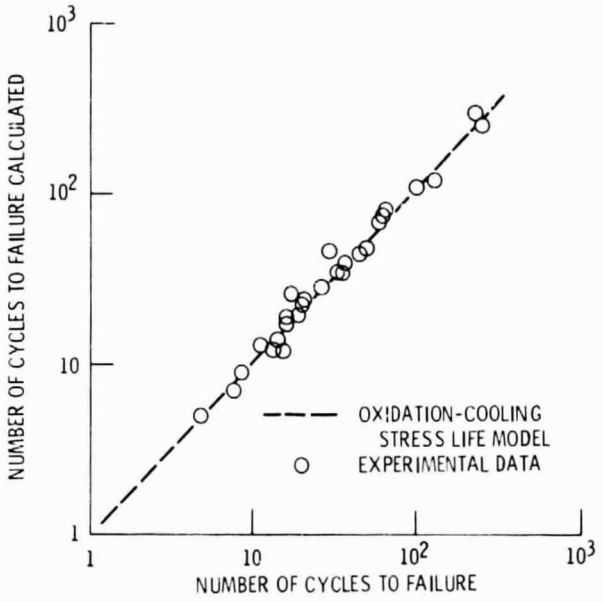

Confirmation of oxidation-cooling stress life model

with the lives predicted by the oxidation-cooling stress life model. It was found that the model could be used quite successfully to predict coating life.

Shear Strength Determination in Unidirectional Fiber-Reinforced Composites

To accurately determine the shear strength of a material, the test specimen geometry and loading must be chosen to produce pure shear in the failure region. The Iosipescu shear specimen meets this requirement along the central plane joining the notch tips. For materials exhibiting plastic yielding, failure generally occurs along this central plane since plastic yielding begins at the notch tip. For brittle materials, however, failure may not necessarily occur on this central plane. Finite-element stress analysis of this specimen at Lewis showed that although the shear stresses were largest in the central plane, they were only slightly lower in a region within approximately one-quarter notch width of the notch center. A brittle material containing a distribution of flaws would then be expected to fail in a region of large flaws and large shear stresses; that is, for the Iosipescu specimen, near the central plane but not necessarily on it.

The analysis was confirmed in room-temperature Iosipescu shear tests of graphite/PMR-15 unidirectional composites. The specimen failures were observed in planes parallel to the fibers and near, but not necessarily at, the central plane, as consistent with the prediction from finite-element analysis. Furthermore the maximum shear stress in the failure plane of the specimen determined from finite-element analysis provided a good estimate of the specimen's shear strength.

Improved Strength of High-Pressure-Nitrogen-Sintered Silicon Nitride

High-pressure-nitrogen sintering is used at Lewis to improve the high-temperature strength of silicon nitride ceramics. By sintering at 1000-psi nitrogen overpressures weight losses due to Si_3N_4 decomposition and Si_3N_4-additive interactions are suppressed and sintering temperatures 300 degrees C higher than those possible under 1-atm nitrogen pressure are possible. The higher sintering temperatures also permit the use of more refractory additives, which improves high-temperature strength. The higher temperatures also facilitate sintering by increasing both the fluidity of the silicate liquid

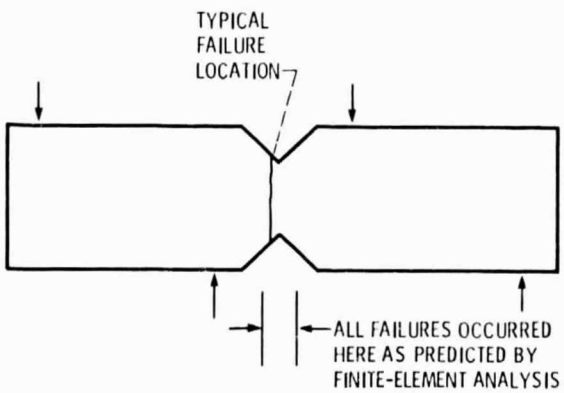

Iosipescu shear specimen

phase and the solutioning of Si_3N_4 in the silicate liquid.

In specially modified high-pressure furnaces capable of 2150 °C, Si_3N_4 test bars with a variety of refractory oxide additives have been sintered to full density. To date, Y_2O_3 produced the greatest strength improvement.

Ductility in Rapidly Solidified NiAl

Aluminide intermetallics, such as NiAl, represent potential structural materials for use at elevated temperatures because they have a high melting point and low density and resist oxidation and high-temperature deformation. However, the potential usefulness of polycrystalline NiAl is limited because it is completely brittle near room temperature. However, recent research at Lewis has shown that NiAl exhibits considerable ductility at 400 °C if the grain size is smaller than approximately 20 μm.

Melt spinning was used in this study to reduce the grain size of NiAl to 5 to 10 μm. Strain to failure in a simple bend test of the melt-spun NiAl ribbon ranged from 0.9 to 2.25 percent. Heat treatment increased the ductility. Fractures ranged from completely intergranular to a mixture of intergranular and transgranular cleavage. Possible explanations for the observed behavior involve the effects of grain size, boundary segregation, and hardening.

Continuing work will include the study of various compositions of NiAl and FeAl and the addition of boron as a grain boundary strengthener.

Low-Wear Fluorinated Polyimides

Tribological studies have been conducted on five different polyimide solid bodies formulated from diamine 2,2-bis [4-(4-aminophenoxy)phenyl] hexafluoropropane (4-BDAF), dianhydride pyromellitic acid (PMDA), and benzophenonetetracarboxylic acid (BTDA).

Friction coefficients, polyimide wear rates, polyimide surface morphology, and transfer films were evaluated at sliding speeds of 0.31 to 11.6 m/s at temperatures from 25 to 300 °C. The tribological properties were highly dependent on the composition of the polyimide and on the experimental conditions. Two of the polyimides produced very low wear rates but very high friction coefficients (greater than 0.85) under ambient conditions. They offer considerable potential for high-traction applications such as brakes and traction drives.

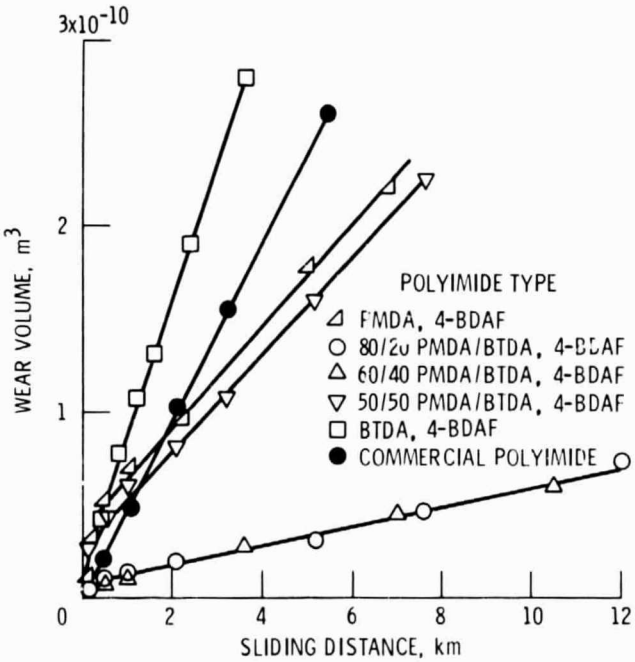

Polyimide wear volume

Title	Lewis contact	Phone number, (216) 433-4000, extension—	Headquarters program office
Passive Eddy Current Damper Technology for Cryogenic Machinery	Albert F. Kascak	6117	OAST
Swept-Fan-Blade Flutter	Robert E. Kielb	5104	OAST
Photo-Optical Blade Vibration Data Acquisition System	L. James Kiraly	6950	OAST
Effects of Different Rub Models on Gas Turbine Rotor Dynamics	Albert F. Kascak	6117	OAST
High-Temperature Erosion Rig	Robert F. Handschuh	6895	OAST
Method for Fabricating All-Zirconia Gas Path Seals	James D. Cawley	6895	OAST
Nondestructive Characterization of Structural Ceramics	Alex Vary	357	OAST
Structural Dynamics Code for Entire Turbine Engines	Gerald V. Brown	5368	OAST
New Method of Power Transmission Shaft Design	Stuart H. Loewenthal	6839	OAST
Analytical Method to Predict Aircraft Gearbox Efficiency	Stuart H. Loewenthal	6839	OAST
Nonlinear Analysis for High-Temperature, Multilayered Fiber Composite Structures	Dale A. Hopkins	6272	OAST
Interply Layer Effects on "Free Edge" Stress Field	Christos C. Chamis	5103	OAST
Dynamic Stress Analysis of Smooth and Notched Fiber Composites	Christos C. Chamis	5103	OAST
Simplified Composite Micromechanics Equations	Christos C. Chamis	5103	OAST
Linear Approximations to Three-Dimensional Inelastic Analysis	Christos C. Chamis	5103	OAST
Interply-Layer Progressive Degradation Effects	Christos C. Chamis	5103	OAST
ICAN: Integrated Composite Analyzer	Christos C. Chamis	5103	OAST
Select Composites for Space Applications: A Mechanistic Assessment	Carol A. Ginty	6831	OAST
Finite-Element Substructuring for Composite Micromechanics	John J. Caruso	6831	OAST
Progressive Fracture of Fiber Composites	Thomas B. Irvine	6272	OAST
Lower Curing Temperature for PMR Polyimides	Peter Delvigs	6163	OAST
Better Understanding of Friction and Wear Properties of Ferrites	Kazuhisa Miyoshi	5271	OAST
Surface Roughness Effects in Elastohydrodynamic Contacts	Bernard J. Hamrock	6151	OAST
Oxidation/Corrosion Study of Stirling Engine Alloys	Joseph R. Stephens Charles A. Barrett	6676 6617	OAST
Super Single-Crystal Superalloys	Rebecca A. MacKay	267	OAST
Life Prediction Model for Advanced Thermal Barrier Coatings	Robert A. Miller	6641	OAST
Shear Strength Determination in Unidirectional Fiber-Reinforced Composites	Frances I. Hurwitz Donald R. Behrendt	6826 6603	OAST
Improved Strength of High-Pressure-Nitrogen-Sintered Silicon Nitride	William A. Sanders Diane M. Mieskowski	5362 5362	OAST
Ductility in Rapidly Solidified NiAl	Darrell J. Gaydash Robert W. Jech Robert H. Titran	712 6293 5213	OAST
Low-Wear Fluorinated Polyimides	Robert L. Fusaro	6118	OAST